THESIS FOR THE DEGREE OF DOCTOR OF PHILOSOPHY (PHD)

Role of AMPK in the regulation of breast cancer metabolism and beige adipocyte differentiation

by

Tamás Fodor

Supervisor: Péter Bay, PhD, DSc

UNIVERSITY OF DEBRECEN

DOCTORAL SCHOOL OF MOLECULAR MEDICINE

DEBRECEN, 2018.

TABLE OF CONTENTS

ABBREVIATIONS

ACC	acetyl-CoA carboxylase
ACO2	aconitase-2
AgRP	agouti related neuropeptide
AICAR	5-Aminoimidazole-4-carboxamide 1-β-D-ribofuranoside
AMP	adenosine monophosphate
AMPK	AMP-activated kinase
ANOVA	analysis of variance
ATP	adenosine triphosphate
ATP5g1	ATP synthase lipid binding protein
BAT	brown adipose tissue
BMP4	bone morphogenetic protein 4
CaMKKβ	Ca^{2+}-calmodulin-dependent kinase kinase
CIDEA	cell-death-inducing DNA fragmentation factor-*α*-like effector A
CMF	Cyclophosphamide Methotrexate Fluorouracil
CPT-1	carnitine palmitoyltransferase-1
DioC6	3,3′-dihexyloxacarbocyanine iodide
DMEM	Dulbecco's modified Eagle's medium
ECAR	extracellular acidification rate;
FGF21	fibroblast growth factor 21
FOXO	forkhead box O
GLP-1	glucagon-like peptide-1
GS	glycogen synthase
hADMSCs	human adipose tissue-derived mesenchymal stem cells
HIF	hypoxia inducible factor
IDH2	isocitrate dehydrogenase-2
LKB1	liver kinase B1
MAPKK	Mitogen-activated protein kinase
MTX	methotrexate
mTOR	mechanistic target of rapamycin
NAD^+/NADH	Nicotinamide adenine dinucleotide
NAMPT	nicotinamide phosphoribosyl transferase
NRF	nuclear respiratory factor
NRG4	neuregulin 4
OCR	oxygen consumption rate

pACC	phospho-acetyl-CoA carboxylase
PBS	Phosphate Buffered Saline
PGC1α	peroxisome proliferator activated receptor-γ cofactor-1 α
PPARγ	peroxisome proliferator activated receptor γ
PRDM16	PR domain containing16
RT-qPCR	reverse transcription-coupled polymerase chain reaction
SDS-PAGE	sodium dodecyl sulfate-polyacrylamide gel electrophoresis
SIRT1	sirtuin 1
SRB	sulphoradamine B
TAK1	transforming growth factor-1-activated kinase
TBX-1	T-box protein 1
TCA	tricarboxylic acid
TCAA	tricarboxylic acetic acid
TMEM26	transmembrane protein 26
UCP1	uncoupling protein 1
ZMP	5-aminoimidazole-4-carboxiamide-1-D-ribofuranosyl-5'-monophosphate
WAT	white adipose tissue

1. INTRODUCTION

Living organisms must accommodate to changes in the environment, the availability or scarcity of nutrients and to changes of the external temperature. Therefore, cells possess an energy and nutrient sensor system that fine-tunes metabolism to meet the needs of the organism. The pathological function of this sensory system leads to a pathological metabolic adaptation that may in fact contribute to carcinogenesis and cancer progression. My dissertation presents two studies that assess the regulation of both physiological and pathological metabolic adaptation.

2.1 AMPK as a metabolic regulator in health and disease

Every organism faces continuously with energy demands during their lifetime. In response to these initiator stress factors cells evolved complex metabolic processes to be able to stock fuel substrates when food source is ample and to be able to reduce energy consumption and mobilize stores when food is scarce. These energy balancing processes are essential for survival in both short term and prolonged nutrient deprivation (Viollet et al. 2010).

5'-adenosine monophosphate (AMP)-activated protein kinase called AMPK is a well-studied heterotrimeric enzyme complex, a Ser/Thr kinase with prominent role in the maintenance of cellular energy equilibrium in mammalian cells. AMPK is sensitive for alterations in the energy charge reflected by changes in the ATP/AMP ratio. When AMPK is activated by the decreased ATP/AMP ratio, it switches on catabolic mechanisms while simultaneously switching off anabolic processes to rebalance the energy state (Hardie 2007) (Figure 1).

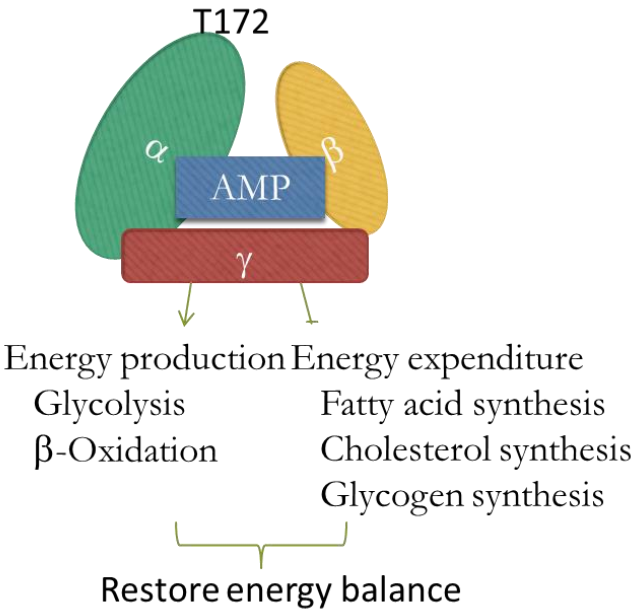

Figure 1. AMP activated protein kinase (AMPK) is an energy sensor that regulates cellular metabolism

AMPK is a heterotrimeric complex consisting of the catalytic α subunit and the non-catalytic β and γ subunits. When activated by a deficit in nutrients, AMPK stimulates mitochondrial energy production, while turning off energy-consuming processes to restore energy balance. Figure reproduced from (Long and Zierath 2006).

Besides these protective effects AMPK has diverse role in detecting and regulating not only the metabolism of peripheral tissues (e.g. adipose tissue, liver, pancreatic β cells, skeletal muscle) but also energy sensing in the central nervous system, more closely, the hypothalamus and hence fine-tunes the whole body energy homeostasis. Moreover, AMPK is downregulated in most common chronic diseases like cancer, diabetes, inflammation, and obesity. Due to these facts, AMPK became a possible therapeutic target in the above mentioned diseases.

2.2 The role of AMPK in the switch towards Warburg metabolism

Otto Warburg revealed that cancer cells have different metabolism as compared to normal, non-transformed cells. He hypothesized that this reprogrammed metabolism is the essential cause of cancer (Warburg, Wind, and Negelein 1927). The Warburg effect can be identified in most cancer cells, among others, in breast cancer, where ATP production via glycolysis s is the main energy source even under aerobic condition. Furthermore, these cells are characterized by downregulated mitochondrial oxidation and elevated flux of glycolysis with higher lactate production rate and pentose phosphate shunt in order to support rapid cell proliferation. Cancer cells consume high volume of glucose and glutamine from external

source and utilize glycogen as an internal substrate source (Wallace 2012; Favaro et al. 2012). Elevated glycolytic rate can also boost the pentose phosphate pathway that enhances the de novo nucleotide synthesis (Icard and Lincet 2012).

In tumor cells glycolysis and the TCA cycle are uncoupled. In the cytosol glycolysis provides intermediates for the pentose phosphate shunt to support nucleotide production. Meanwhile, in the mitochondria, the TCA cycle uses glutamine for citrate production via alternative enzymes further supporting uncontrolled cell proliferation (Wallace 2012) (Figure 2).

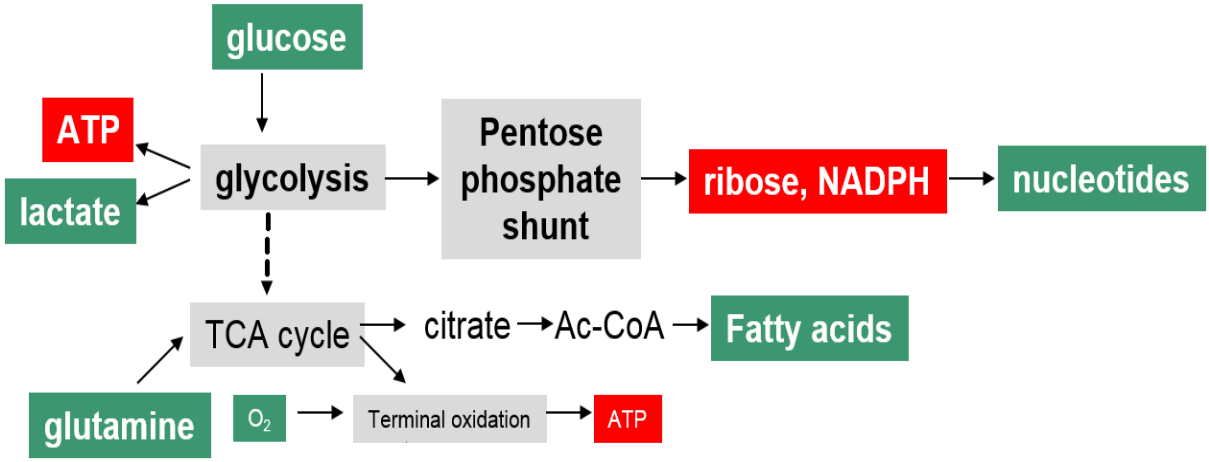

Figure 2. Main characteristics of the Warburg effect

In cancer cells metabolic reprograming increases the rate of aerobic glycolysis, furthermore, glycolysis and the TCA cycle uncouples. Glycolysis supplies the pentose phosphate shunt with intermediers for nucleotide synthesis while the TCA cycle is charged from alternative sources, such as glutamine, to produce citrate for fatty acid synthesis. In our experiments we inhibited nucleotide synthesis by the folate analog methotrexate (MTX) and used AICAR to stimulate AMPK.

With regard to rapid cell division, it is important to emphasize that the G1/S checkpoint is under metabolic control. Any interruption to the metabolism blocks the cell cycle at the G1 to S transition (Green, Galluzzi, and Kroemer 2014). AMPK has intricate connections with other metabolic and energy sensing pathways like Akt, mTOR, SIRT1 and PARPs (Hardie 2007; Bai et al. 2015; Hsu and Sabatini 2008). Upon AMPK activation mitochondrial oxidation, and consequently mitochondrial biogenesis enhances, which had been related to anti-Warburg and antiproliferative effect on lymphomas (Faubert et al. 2013).

To assess the possible role of AMPK in reverting Warburg metabolism and to investigate its antiproliferative effect we applied 5-aminoimidazole-4-carboxiamide 1-β-ribofuranoside (AICAR), a pharmacological activator of AMPK and the folate-dependent 1-carbon metabolism analog, nucleotide synthesis inhibitor methotrexate (MTX) (Sullivan et al. 1994) (Figure 2).

In our study, as an in vitro model, we used MCF7 breast cancer cells. Breast cancer is the most common cancer in women worldwide with close to 1.7 million new cases diagnosed in 2012. This represents about 12% of all new cancer cases and 25% of all cancers in women. Despite of the extensive prevention programs, it is still the fifth most common cause of death from cancer in women (Ferlay et al. 2015).

Breast cancer cell metabolism is described by Warburg rearrangements and more importantly, endeavors to revert Warburg metabolism support chemotherapy (Suhane and Ramanujan 2011; Feng et al. 2014; Ayyasamy et al. 2011). MTX can inhibit *de novo* nucleotide synthesis by hampering the folate–dependent 1 carbon metabolism. Methotrexate acts specifically during DNA and RNA synthesis, and thus it is cytotoxic during the S-phase of the cell cycle. In breast cancer chemotherapy treatment MTX is used in combination with cyclophosphamide and 5-fluoro-uracil that is called CMF protocol (Bevers et al. 2009).

The obvious relevance of Warburg metabolism in breast cancer suggested that the anti-Warburg metabolic rearrangements upon AMPK induction may have an antiproliferative effect and possibly act synergistically with methotrexate.

2.3 The role of AMPK in beige adipocyte physiology

The energy homeostasis of living organisms is determined by energy input and energy consumption. Any acute or long term disturbance to the energy balance leads to chronic metabolic diseases (Houtkooper, Pirinen, and Auwerx 2012; Verdin et al. 2010). Energy dissipation depends on the energy generated by the active biochemical processes (e.g. phosphorylation-dephosphorylation), physical exercise and mitochondrial oxidative phosphorylation (e.g. cardiac and skeletal muscle or brown adipose tissue) (Auwerx 2006).

Adipose tissue has a fundamental role in maintaining organismal energy balance. There are three types of adipose tissues: white adipose tissue (WAT), brown adipose tissue (BAT) and the beige adipose tissue (merged of brown and white). WAT is the main adipose tissue in mammals with a function of storing excess energy. BAT and beige adipocytes have similar functions in rodents and mammals. Both of them have thermogenic capacity to break down glucose and fat and produce heat via the activation of uncoupling protein 1 (UCP1) which uncouples cellular respiration and mitochondrial ATP synthesis (Inagaki, Sakai, and Kajimura 2017).

Upon adrenergic activation beige adipocytes enhance lipolysis, mitochondrial oxidation, mitochondrial biogenesis and the creatin-phosphate cycle (Wu et al. 2012; Petrovic et al. 2010; Kazak et al. 2015). Several factors are able to induce beige differentiation and browning such as environmental stress, hormones, and inflammation. Functionally active and transplantable beige cells were found in humans and it is plausible to assume that beige

adipocytes have similar proportions in heat generation as the skeletal muscle tissue (Pyrzak, Demkow, and Kucharska 2015; Wu et al. 2012). Hormones such as irisin, BMP4, FGF_{21}, GLP-1, NRG4 with the signal of AgRP neurons and the serotoninergic system can stimulate beige differentiation and browning (Wu et al. 2012; Fu et al. 2014; Christian 2015; Gustafson et al. 2015; Lopez, Dieguez, and Nogueiras 2015; Ruan et al. 2014; McGlashon et al. 2015) (Figure 3).

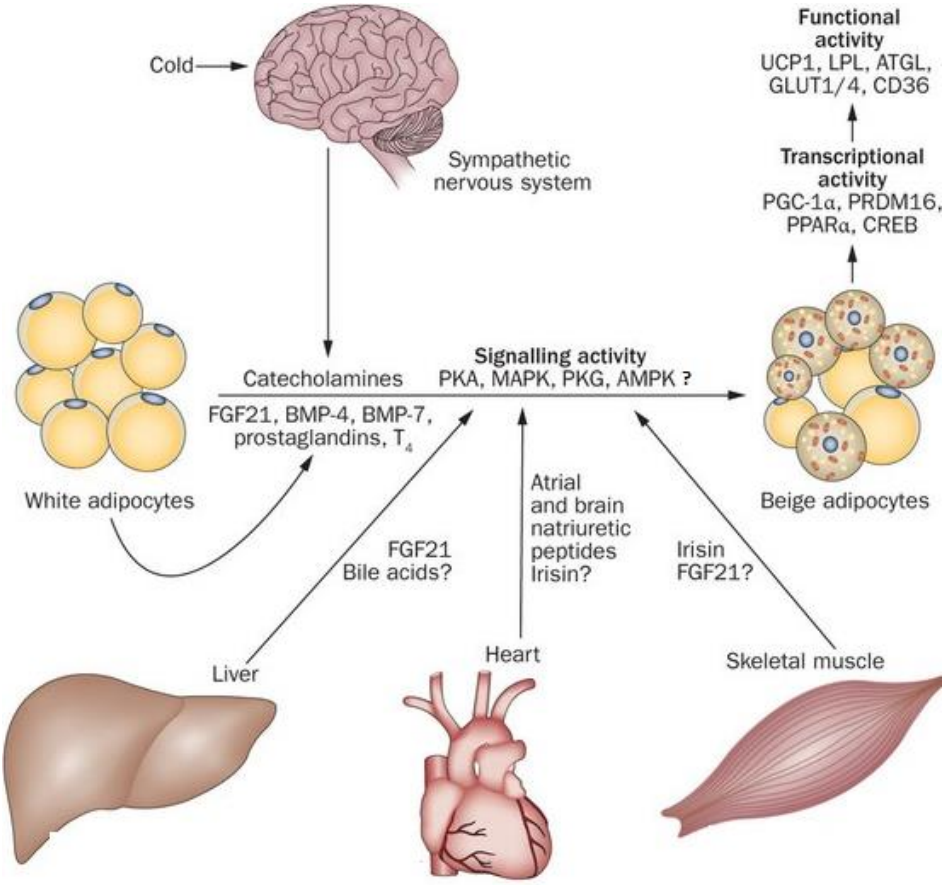

Figure 3. Hormonal control of browning

The metabolically active organs release endocrine and paracrine hormones which are able to regulate the metabolic adaptation of the body to environmental stresses, like cold exposure and altered metabolic situations such as exercise, fasting, feeding and obesity. The sympathetic nervous system releases catecholamines as a response to cold exposure which plays a key role in the activation of energy sensing pathways, not only in white but also in beige adipocyte precursors. These metabolic activities enhance the expression of transcriptional factors which in turn lead to the generation of a beige like phenotype and the characteristics of the beige adipocytes such as increase in energy uptake, energy processing and energy expenditure. Modified figure from (Bartelt and Heeren 2014).

It is important to note that fibrates or thiazolidinediones can also induce browning (McGlashon et al. 2015; Qiang et al. 2012). Activation of beige adipocytes induce sirtuin 1 (SIRT1) that in turn deacetylates PPARγ that boosts peroxisome proliferator activated receptor cofactor-1α (PGC1α) which results in elevated level of mitochondrial oxidation and mitochondrial biogenesis (Qiang et al. 2012).

AMPK is not only an upstream regulator of SIRT1 (Canto et al. 2009) and a master regulator of energy balance, but is also known to play role in brown adipose tissue differentiation through inducing mitochondrial oxidation and mitochondrial biogenesis (Vila-Bedmar, Lorenzo, and Fernandez-Veledo 2010).

It is therefore very likely that AMPK can also affect beige adipose tissue differentiation via the activation and enhancement of mitochondrial activity and mitochondrial biogenesis. Thus, we aimed to explore these functional and metabolic processes.

3. REVIEW OF THE LITERATURE

3.1 Regulation of AMPK

3.1.1 Structure of AMPK

Cells continuously need an optimized energy state that is necessary to maintain the cellular energy homeostasis which is essential for cell survival. Therefore, ATP utilization and production needs to be balanced. The major energy sensor that enables sensing of the AMP to ATP ratio is the 5' adenosine monophosphate-activated protein kinase (AMPK) (Hardie 2007). The most notable feature of AMPK is its sensitivity to the cellular energy state. Decreases in the ATP/AMP ratio can activate AMPK through interdependent allosteric and post translational modifications (Jeon 2016). AMPK is a heterotrimeric enzyme complex made up of the catalytic α and the regulatory β and γ subunits all of which are necessary for AMPK activity. There are different isoforms of the α, β and γ subunits, namely, α1, α2, β1, β2 and γ1, γ2 and γ3, respectively. Nevertheless, due to alternative splicing other isoforms exist, too. In mammals, these isoforms are coded by seven genes. The α and β subunits are encoded by two genes namely PRKAA1, PRKAA2 and PRKAB1, PRKAB2, while the γ subunit is encoded by an additional three genes PRKAG1, PRKAG2 and PRKAG3 (Long and Zierath 2006). The α1, β1, and γ1 (the common isoforms) are expressed in most mammals cells. The α2, β2, γ2, and γ3 isoforms are abundant in cardiac and skeletal muscle. The γ-subunit has the major role in direct sensing and binding with cytoplasmic AMP/ADP in order to stimulate the enzymatic activity of AMPK (Moffat and Harper 2010). The γ subunit has four cystathionine beta synthase (CBS) domains which provide AMPK with the capability to sensitively detect the alterations in the AMP/ATP ratio. (Figure 4).

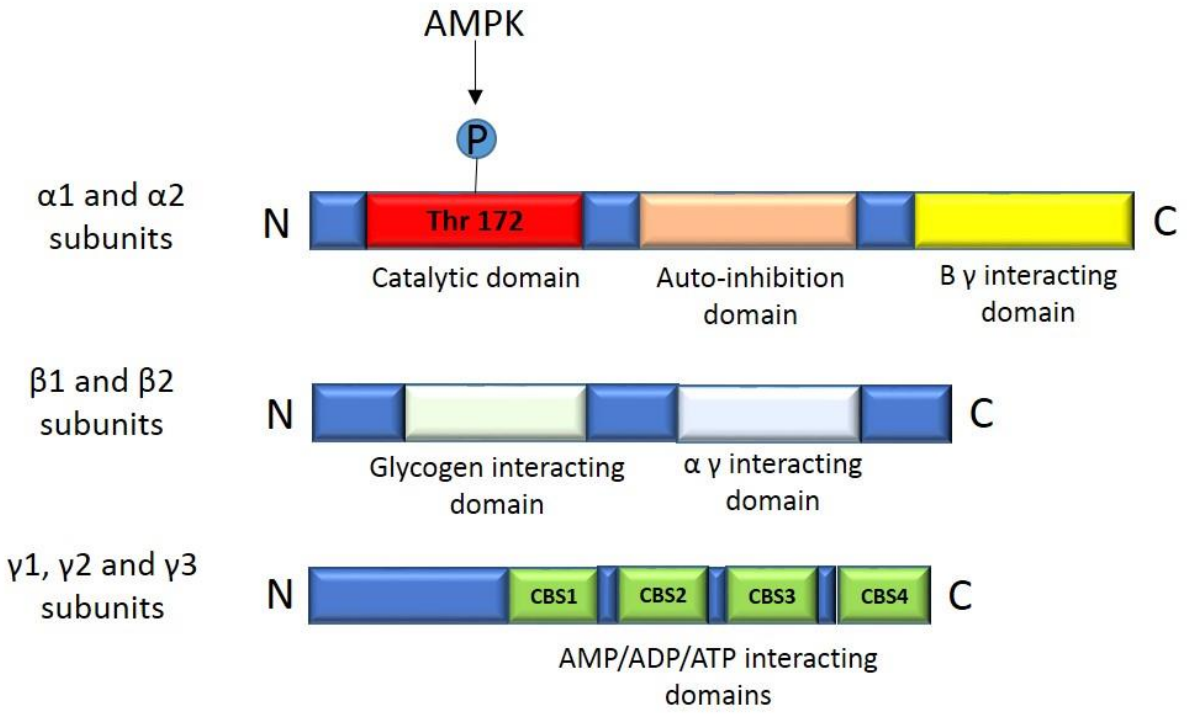

Figure 4. Structure of AMP-activated protein kinase (AMPK)

AMPK consists of three subunits: the catalytic subunit (AMPK-α) and two regulatory subunits (AMPK-β and AMPK-γ). On the α subunit we can find a catalytic domain at the N-terminal where the enzyme can be phosphorylated by upstream kinases at Thr172. The auto-inhibition domain and β, γ interacting domains are situated on the α subunit. The β subunit includes the glycogen and α, γ interacting domains. The γ regulatory subunit consists of four cystathionine β synthase (CBS) domains which have a vital role in the interaction with AMP, ADP and ATP. Modified figure from (Sanchez et al. 2012).

AMPK is activated when metabolic balance is perturbed by a deficit of nutrient energy. Consequently AMPK turns on ATP-generating processes (stimulation of hepatic fatty acid oxidation, ketogenesis, stimulation of skeletal muscle fatty acid oxidation and glucose uptake), meanwhile it switches off ATP consuming processes (inhibition of cholesterol synthesis, lipogenesis, and triglyceride synthesis, inhibition of adipocyte lipolysis and lipogenesis, and inhibition of insulin secretion by pancreatic beta-cells (Winder and Hardie 1999).

3.1.2. Regulation of AMPK by the AMP/ATP ratio

In an energetically quiescent cell, the ATP/ADP ratio is 10:1 and the ATP/AMP ratio is 100:1. Energetically unfavorable reactions require high ATP/ADP ratio. Elevated levels of ATP consumption which are not covered by sufficient ATP production will lead to an increment of ADP. ADP will be quickly converted to ATP and AMP by adenylate kinases in the following reaction:

$$2ADP \leftrightarrow ATP + AMP$$

This reaction dramatically increases AMP levels and consequently AMP boosts the activity of AMPK by 5-fold (Adams et al. 2004). The activation of AMPK takes place at the *γ*-subunit, at the AMP binding site. Increased AMP concentration will lead to conformational alterations of the γ-subunit that will allow two AMP molecules to connect to the four Cystathione beta synthase (CBS) domains which also referred to as Bateman domains. This conformational change leads to a moderate increase in AMPK activity about 2- to 10-fold. This change also enhances the phosphorylation of Thr172 of the α-subunit, which further activates AMPK. The phosphorylation of AMPK results in an additional activation leading to an at least 100-fold increase in its activity (Hardie and Alessi 2013). Interestingly, a recent study pointed out that AMPK is also regulated by ADP and not only by AMP and ATP (Xiao et al. 2011). (Figure 5).

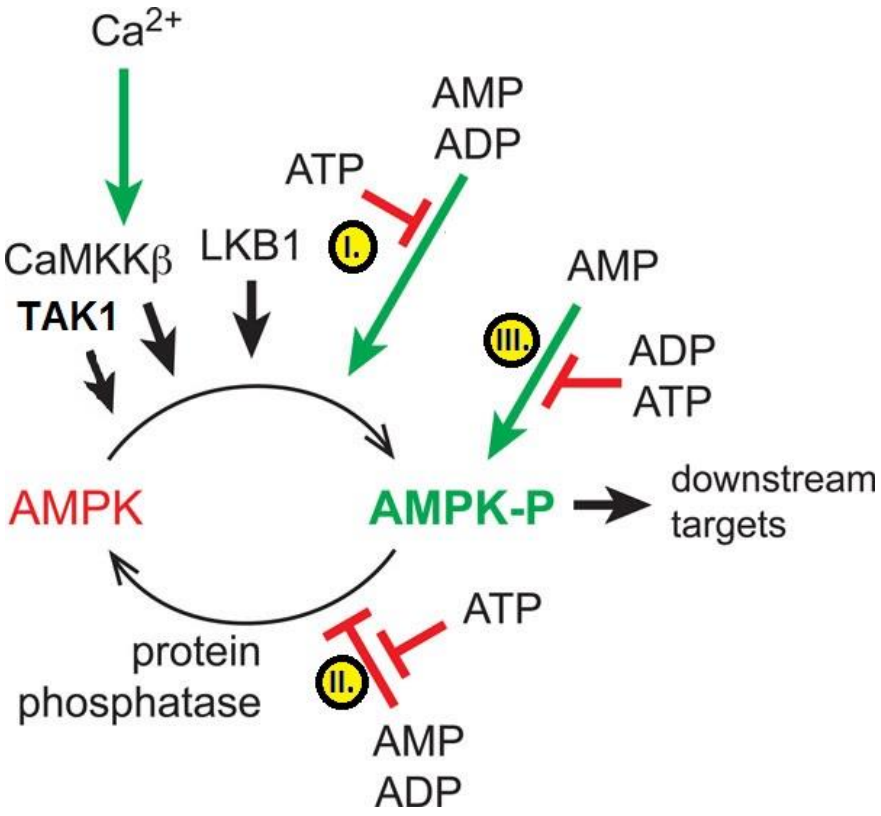

Figure 5. Mechanisms for activation of AMPK by AMP

AMPK can be activated by increment in cellular AMP/ATP or ADP/ATP ratios, as well as by upstream kinases (CaMKK, LKB1, TAK1). AMPK activity is enhanced by more than 200–fold upon phosphorylation at Thr172. This process is catalyzed by upstream kinases. The alteration in ADP or AMP level activates AMPK via three possible mechanisms: 1) The binding of ADP or AMP to AMPK results conformational changes which direct support phosphorylation by upstream kinases. 2) The binding of ADP or AMP to AMPK causes conformational changes that inhibits dephosphorylation by protein phosphatases. 3) When only AMP is binding but not ADP, it causes the allosteric activation of AMPK-P. These AMPK activation pathways are antagonized by ATP and support AMPK to behave as a master energy regulator. Modified figure from (Hardie and Alessi 2013).

3.1.3 AMPK activation by upstream kinases

There are several upstream kinases that can activate AMPK (Figure 7). One such kinase is the serine-threonine liver kinase B1 (LKB1) that is necessary for the activation of AMPK in response to stress. LKB1 is encoded by the Peutz-Jeghers syndrome tumor suppressor gene. This enzyme remains structurally conserved across species, playing a vital role in mediating metabolic homeostasis, cell multiplicity, polarity and autophagy initiation (Andrade-Vieira et al. 2014). LKB1 has been described as a tumor suppressor. Since its loss-of-function mutation is commonly detected and believed to directly induce the oncogenesis in a wide range of malignancies. E.g. in Peutz-Jeghers syndrome that is associated with hamartomas located in the gastrointestinal tract with higher risk of transforming into invasive

malignancies than sporadic polyps. Moreover LKB1 harbors germline mutations genes in lung, breast, cervical, pancreatic, biliary and testicular cancers (Gan and Li 2014).

For the activation of LKB1, Ste-20 related adaptor (STRAD) and mouse protein 25 (MO25) needs to bind to LKB1 building up a heterotrimeric kinase. This holoenzyme complex is also referred as LKB1-STRAD-MO25. It ultimately translocates into the cytoplasm and acts as a regulatory kinase to phosphorylate a spectrum of its downstream targets, including AMPK (Korsse, Peppelenbosch, and van Veelen 2013). LKB1 activates AMPK by phosphorylating the α-catalytic subunit at the threonine residue 172. The activation of AMPK by LKB1 is mainly dependent on the AMP/ATP ratio (Carling, Sanders, and Woods 2008).

The second notable AMPKK is the Ca^{2+}-calmodulin-dependent kinase (CaMKK2). It is one of the kinases which phosphorylates, and in turn activates AMPK in response to increased intracellular calcium levels without any detectable changes in the AMP/ATP ratio. The CaMKK2 is expressed mainly in the brain and to a lower extent in the liver, skeletal muscle, testes, thymus and T-cells (Birnbaum 2005). Higher CAMKK2 expression was observed in gastric and prostate cancer and connected to potentiating gastric and prostate cancer cells for proliferation and invasion through phosphorylating and AMPK activation (Subbannayya et al. 2015).

The third upstream kinase of AMPK is the transforming growth factor-1-activated kinase (TAK1) that is a member of MAP kinase kinase kinase (MAPKKK) family. TAK1 also has an AMPK activating effect by directly phosphorylating the Thr172 residue of AMPK. AMPK can reciprocally activate TAK1, creating a feedback loop (Kim et al. 2012). Although, those physiological conditions under which TAK1 can phosphorylate AMPK are unclear yet (Momcilovic, Hong, and Carlson 2006), the activation of the TAK1/AMPK signaling axis plays essential roles in protecting against malignant expansion and inducing protective autophagy in pancreatic cancer or hepatocellular carcinoma (Inokuchi-Shimizu et al. 2014; Kim et al. 2012; Wang et al. 2013).

The phosphorylated Thr172 residue can be dephosphorylated by protein phosphatases. Among protein phosphatases, PP2A and PP2C can dephosphorylate AMPK which in turn inhibits AMPK activation (Davies et al. 1995; Sanders et al. 2007) (Figure 6).

A new study pointed out that ubiquitin-dependent proteasome degradation mediated by CIDEA (cell-death-inducing DNA fragmentation factor-*α*-like effector A) is able to regulate AMPK activity (Qi et al. 2008) and in line with that, a CIDEA-binding site has been identified on the AMPK *β*-subunit (Qi et al. 2008). In addition to that, AMPK *β*-myristoylation has a central role in AMPK phosphorylation and activation by upstream kinases in response to metabolic stress signals (Oakhill et al. 2010).

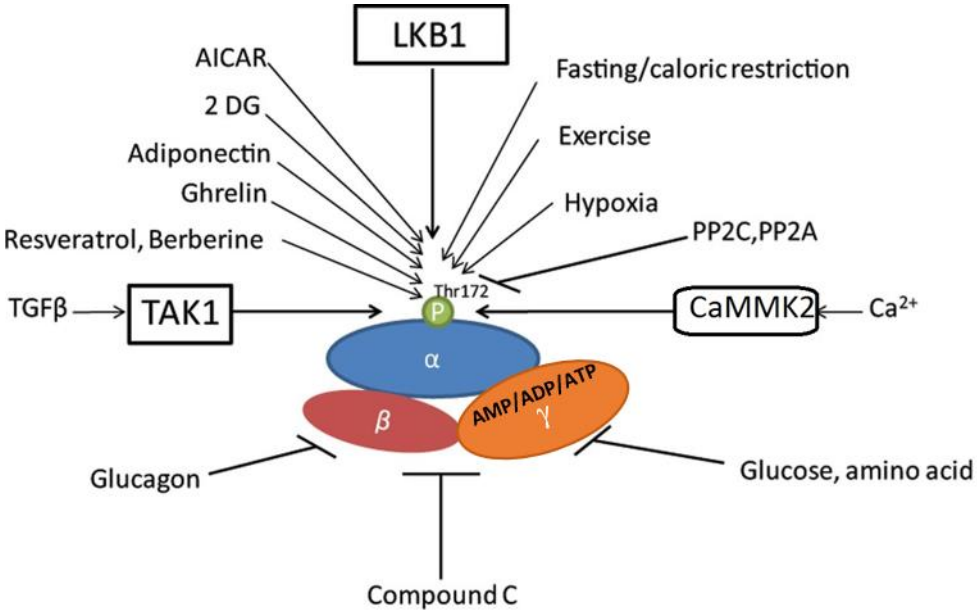

Figure 6. The role of AMP-activated protein kinase in stress responses

Modified figure originated from (Wang, Song, and Zou 2012).

3.2 Activation of AMPK in Physiological and Pathological Conditions

3.2.1 AMPK Activators

AMPK acts as an energy sensor by sensing the AMP/ATP ratio. Therefore, AMPK activation under physiological conditions aims to restore energy balance in metabolic or energetic crisis where ATP content is compromised like in hypoxia, ischemia, low nutrient status or when ATP consumption is elevated. As a consequence, AMPK activation initiates catabolic processes to generate ATP and suppresses ATP consuming processes that are not necessary for the immediate survival of the cell (Canto and Auwerx 2010) (Figure 7).

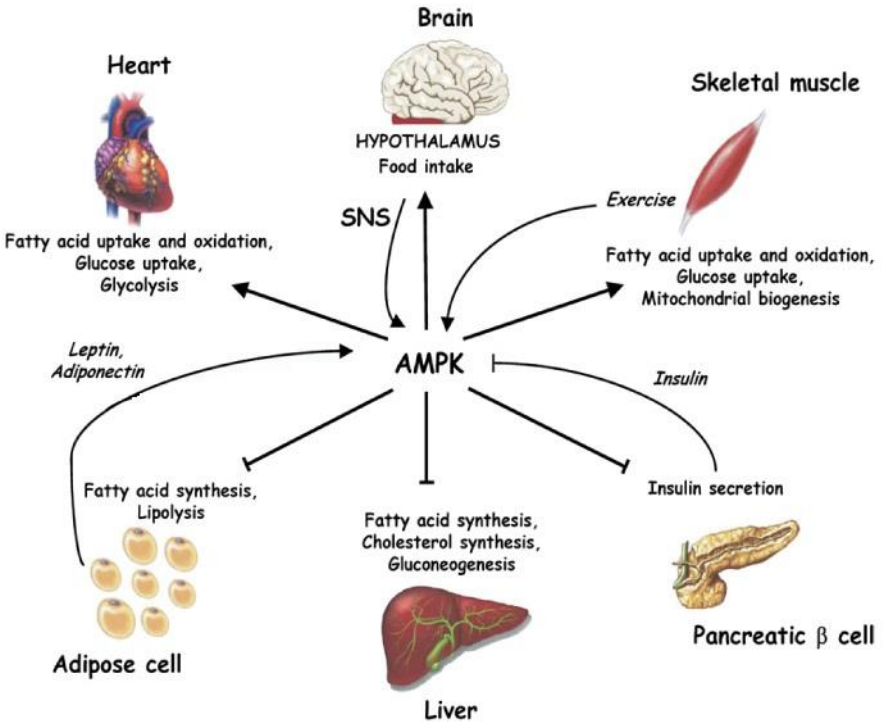

Figure 7. Roles of AMPK in the control of whole-body energy homeostasis
Modified figure from (Kahn et al. 2005)

Plenty of natural drugs, plant compounds, several hormones and artificial drugs are able to activate AMPK. We can distinguish four classes based on their mechanism of action (Figure 8).

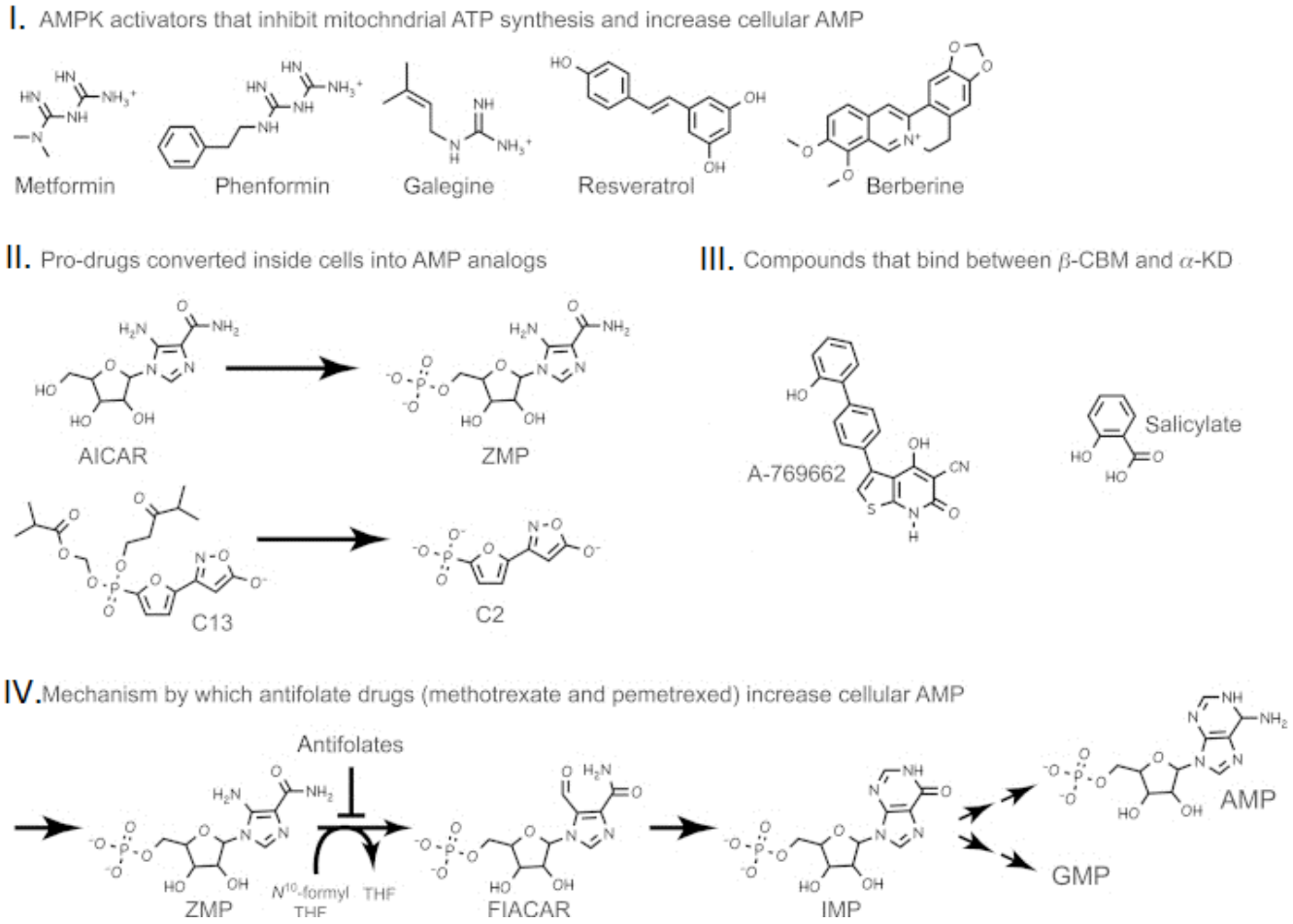

Figure 8. AMPK activators based on their mechanism of action

Regulation of AMP-activated protein kinase by natural and synthetic activators. Modified figure taken from (Hardie 2016).

The first group of activators acts indirectly via the inhibition of the mitochondrial ATP synthesis either through inhibiting Complex I (*e.g.*, metformin or phenformin), Complex III (*e.g.*, antimycin A) or the mitochondrial F1 ATP synthase (*e.g.*, oligomycin) in the respiratory chain. All of these compounds also increase cellular ADP/ATP and AMP/ATP ratios, although correlations between such ratios and changes in AMPK activity do not prove that AMPK activation by AMP or ADP is the only mechanism of activation (Hardie 2016).

The second group of activators are the pro-drugs that are converted inside the cells to AMP analogs, such as 5-aminoimidazole-4-carboxiamide riboside (AICAR). In our studies we applied AICAR to induce AMPK activation. AICAR is taken up by adenosine transporters and it is consequently phosphorylated by intracellular adenosine kinase to 5-aminoimidazole-4-carboxiamide-1-D-ribofuranosyl-5'-monophosphate (ZMP). ZMP is an AMP mimetic that binds to AMPK exactly at the same sites as AMP and has the same effect on the activation of AMPK as AMP does (Corton et al. 1995).

The third group consists of allosteric activators which bind directly to AMPK at sites distinct from AMP sites. A natural compound, salicylate, an aspirin metabolite is an example of these agents (Amann and Peskar 2002) (Hawley et al. 2012).

The fourth group is where the antifolate drugs are able to activate AMPK via ZMP accumulation.

In addition some physiological hormones possess similar activating effects on AMPK as the previously listed drugs. One of these hormones is leptin that is secreted by adipocytes in the presence of insulin. Leptin regulates the energy balance by inducing satiety. In peripheral tissues, such as skeletal muscle, leptin can directly activate AMPK by ameliorating the AMP/ATP ratio (Minokoshi et al. 2002). A recent study pointed out that the antimetabolite methotrexate, which we also used combined with AICAR in our study, dramatically sensitizes cells to the activating effects of AICAR and showed a remarkable additive effect (Pirkmajer et al. 2015).

3.2.2 AMPK effects, downstream targets

There are several consequences of the AMPK activation at the organism level. One example of these is the increase in glucose uptake by skeletal muscle via the induction of GLUT4 translocation to the plasma membrane (Kurth-Kraczek et al. 1999). Downstream, AMPK activation can enhance glycolytic flux as a consequence of the phosphorylation of Ser466 and activation of 6-phosphofurcto-2-kinase (PFK-2). Enhanced glycolytic flux contributes to AMPK-mediated ATP generation (Carling and Hardie 1989; Marsin et al. 2000). At the same time, AMPK decreases glycogen synthesis rate through phosphorylating glycogen synthase (GS) at Ser7, which inhibits its activity and further shunts glucose into glycolysis (Halse et al. 2003).

AMPK can counteract energy deficit through the activation of fatty acid oxidation. To that end AMPK phosphorylates both isoforms of acetyl–CoA carboxylase (ACC) on Ser79 and Ser212 and inhibits its activity (Hardie and Pan 2002). ACC catalyzes the reaction between malonyl-CoA and acetyl–CoA, which is the first step of the lipid biosynthesis (Hardie and Pan 2002) (Figure 9).

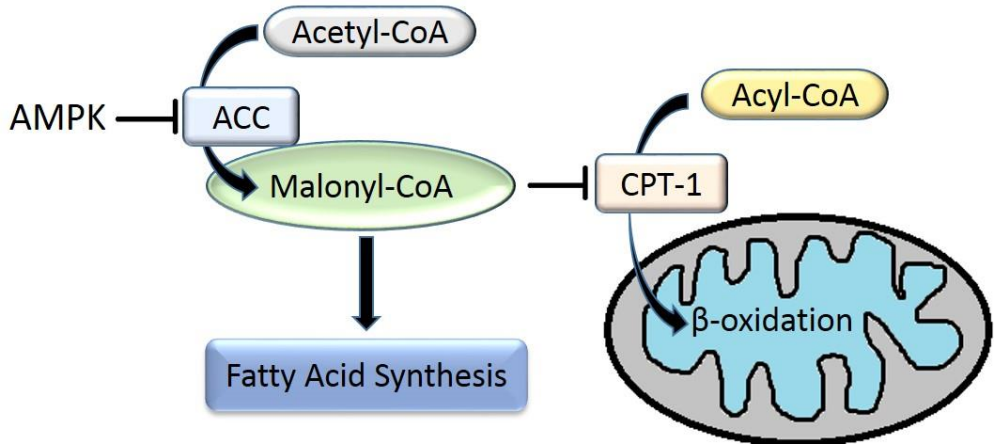

Figure 9. AMPK regulates fatty acid synthesis and β-oxidation

If the cell is in need of ATP, then AMPK inhibits the enzymatic activity of the Acetyl-CoA carboxylase (ACC). ACC catalyzes the carboxylation of acetyl-CoA to malonyl-CoA. Malonyl-CoA allosterically inhibits the carnitine palmitoyltransferase-1 (CPT-1). CPT-1 catalyzes the transfer of fatty acyl groups from Acyl-CoA to carintine and supports the transport from the cytosol to the mitochondria for β-oxidation. This promotes fatty acid oxidation and subsequent generation of mitochondrial ATP. Modified figure from (Lipovka and Konhilas 2015).

ACC phosphorylation by AMPK turns ACC to an inactive state and therefore decreases the rate of fatty acid synthesis and indirectly increases the expression of the fatty acid translocase CPT1b. Together, the elevated rate of glycolysis and β-oxidation are able to activate ATP synthesis to regain the normal energy balance of cells (Mills, Foster, and McGarry 1983).

AMPK has an indirect impact on protein metabolism by blocking the mTOR pathway which is a major inductor of the protein synthesis (Polak and Hall 2009). This escalates via the phosphorylation of TSC2 and raptor, and relies likely on transcriptional events (Polak and Hall 2009).

3.2.3 Role of AMPK in adaptation to hypoxia

In hypoxia the body or a region of the body is deprived of an adequate oxygen supply. Hypoxia occurs under physiological conditions like exhaustive training or pathological conditions such as anemia, hypoventilation, and fibrosis or at locations where oxygen levels are insufficient (e.g. high altitudes).

The inhibition of *β*-oxidation under hypoxia can activate AMPK activation. In non-severe hypoxia ROS (reactive oxygen species) and RNS (reactive nitrogen species) can activate AMPK. ROS/RNS able to activate AMPK through different upstream kinases such as c-Src-mediated PI3K (phosphoinositide 3-kinase) in endothelial cells, or PKC (protein kinase C)-*ζ*. These kinases can phosphorylate LKB1 and hence activate AMPK. H_2O_2, can activate AMPK even in the lack of elevated AMP levels via ROS-dependent CRAC (Ca^{2+} release-activated

Ca^{2+}) channel activation, that can boost cytosolic Ca^{2+} that in turn activates CaMKK2 that can phosphorylate and activate AMPK (Zou et al. 2003; Zou, Shi, and Cohen 2002; Mungai et al. 2011). Finally, AMPK is required for hypoxia inducible factor (HIF) induction in case of hypoxia and an AMPK/HIF1 axis has been prompted to be crucial for cell survival and cell growth under hypoxic condition (Laderoute et al. 2006) (Figure 6).

3.2.4 Role of AMPK in physical exercise

Regular physical training has numerous beneficial effect on health in the prevention and treatment of chronic diseases. Exercise induced muscle contraction is an energy consuming process that may elevate ATP consumption rate about 100 fold and may raise ADP and AMP accumulation, too (Sahlin, Tonkonogi, and Soderlund 1998). In line with that, physical exercise has an insulin-sensitizing effect in which AMPK activation has crucial role.

Intensive muscle contraction initiates the depolarization of T-tubules that induce calcium release from the sarcoplasmic reticulum. Enhanced energy consumption and elevated calcium levels facilitate LKB1-and CaMKK2-regulated AMPK activation (O'Neill 2013). AMPK activation increases fatty acid oxidation and glucose uptake in rat muscles and similar results were obtained in insulin-resistant high-fat-fed rats, pointing out an advantageous possibility to activate AMPK in patients with insulin-resistance or with type 2 diabetes (Merrill et al. 1997). A recent study showed that AMPK activation by AICAR (5-amino-4-imidazolecarboxamide riboside) imitate the effects of training and change the exercise efficiency in a positive manner in mice. Similar experience were noticed in mice treated with peroxisome-proliferator-activated receptor (PPAR) δ activator that also induced AMPK (Narkar et al. 2008; Wang et al. 2004). According to these new findings, AMPK agonists can be considered as exercise mimetics (Narkar et al. 2008) (Figure 6).

3.2.5 Role of AMPK in fasting and caloric restriction

Caloric restriction (CR) can extend the lifespan of yeast, worms, flies, however, in higher order animals, such as in mammals, CR has no effect on lifespan, but can extend health span (Colman et al. 2009). There is AMPK activation upon CR, nevertheless, the importance of AMPK activation in bringing about the beneficial effects of CR has not been proven yet. Several mechanisms of CR mediated AMPK activation have been proposed. Increases in the NAD^+/NADH ratio can activate SIRT1 that in turn deacetylates and activates LBK1 that activates AMPK (Lan et al. 2008). CR-induced decrease in blood insulin can lead to AMPK activation via the decreasing of AKT-mediated phosphorylation on Ser485/491 (Coughlan et al. 2013). Other hormones can also modulate AMPK. Adiponectin in the white adipose tissue (Zhu et al. 2004) or ghrelin in the hypothalamus (Zhu et al. 2004) can activate AMPK. Interestingly, ghrelin is a negative regulator of AMPK in the white adipose tissue and liver

(Kola et al. 2005). Leptin, the “satiety hormone”, has a tissue-specific effect on AMPK. In skeletal muscles it stimulates AMPK activity, meanwhile in the hypothalamus it has a contradictory effect by decreasing hypothalamic AMPK activity (Minokoshi et al. 2002; Minokoshi et al. 2004).

Caloric restriction (CR) or physical exercise can counterbalance 20-40% of the daily nutrient intake that has evident health benefits for humans (Fontana, Partridge, and Longo 2010) (Figure 6).

3.2.6 Interactions between PGC1α and AMPK

The peroxisome proliferator–activated receptor γ co-activator 1α and 1 β (PGC1α and PGC1β) are transcriptional co-regulators which can act as the master regulator of mitochondrial biogenesis and energy expenditure (Vega, Huss, and Kelly 2000). PGC1α regulates several transcription factors such as peroxisome proliferator–activated receptor (PPAR) γ and α (Puigserver et al. 1998; Vega, Huss, and Kelly 2000), estrogen receptor-related α (ERRα) (Huss, Kopp, and Kelly 2002), FOXO1 (Puigserver et al. 2003) and nuclear respiratory factor 1 (NRF1) (Yoon et al. 2001). Through these transcription factors, PGC1α modulates the expression of several genes which has an essential role in gluconeogenesis, fatty acid synthesis and oxidation, glycolysis and other metabolic pathways. PGC1α is responsible for several metabolic functions such as gluconeogenesis in the liver in response to fasting, or increases in mitochondrial biogenesis and respiration in skeletal muscle upon exercise. It seems that PGC1α has a central role in maintaining cellular energy needs and in the case of increased energy consumption.

PGC1β is a homologue of PGC1α. PGC1α and PGC1β have overlapping functions, nevertheless, PGC1β has more restricted role in regulating energy balance as compared to PGC1α (St-Pierre, 2003).

The activity of PGC1α can be regulated by phosphorylation by different upstream kinases such as AMPK, p38, MAPK and Akt. AMPK can phosphorylate PGC1α at Thr177 and Ser538 and hence modulate the co-transcriptional effect of PGC1α (Jager et al. 2007). Moreover, AMPK can increase NAD^+ biogenesis via the Nampt pathway, and therefore boost SIRT1 activity and stimulate the deacetylation and activation of PGC1α (Canto et al. 2009; Fernandez-Marcos and Auwerx 2011).

3.2.7 Interactions between SIRT1 and AMPK

The mammalian sirtuin1 (SIRT1) is a member of the highly conserved NAD^+ dependent class III histon deacetylases and ADP-ribosyltransferase family called sirtuins that consists of seven members (Michan and Sinclair 2007). SIRT1 can be activated by caloric restriction and therefore it has several essential cellular roles, among others, DNA repair, gene

silencing, stress response, aging, metabolic regulation and energy maintenance (Michan and Sinclair 2007; Yu and Auwerx 2009). SIRT1 is able to control glucose, lipid and insulin metabolism in tissues like the brain, skeletal muscle, liver, brown and white adipose tissue or the pancreas (Baur et al. 2010).

SIRT1 can directly regulate the activity of several transcription factors and co-regulators such as PPARγ, p53 and FOXOs transcription factors through deacetylation (Picard et al. 2004; Vaziri et al. 2001; Brunet et al. 2004). Generally, acetylation lowers the activity of these metabolic transcription factors, while under limited energy supply the deacetylation of these enzymes boosts glycolysis, which provides fuel to the TCA cycle and terminal oxidation to meet the energy demand of the cell. SIRT1 can stimulate the mitochondrial biogenesis via the deacetylation and activation of PGC1α (Gerhart-Hines et al. 2007). AMPK activation can induce SIRT1 activity through increasing NAD^+ levels through NAD^+ salvage as described by Nampt (Canto et al. 2009) (Fulco et al. 2008). It is also of note that SIRT1 can produce nicotinamide that is a natural inhibitor of SIRT1 (Bitterman et al. 2002).

3.2.8 Interactions between Foxo1 and AMPK

The family of mammalian forkhead box transcription factors O (FOXOs) has four members: FOXO1, FOXO3, FOXO4, and FOXO6. The FOXO1 and FOXO3 that are expressed in almost all tissues (van der Vos and Coffer 2011). FOXOs has several important roles in cellular metabolism, such as regulation of glucose metabolism, adipogenesis, cellular proliferation, tumor suppression, stress resistance and lifespan extension (Salih and Brunet 2008).

FOXO transcription factors are another downstream targets of AMPK. In nutrient restriction or autophagy FOXOs are regulated by AMPK (Nakashima and Yakabe 2007). AMPK is able to directly phosphorylate FOXO transcription factors at six regulatory sites. The activation of FOXOs by AMPK phosphorylation leads to the upregulation of genes involved in the adaptation to changes in energy metabolism (Greer, Banko, and Brunet 2009).

3.2.9 Basic metabolic changes in cells exhibiting Warburg metabolism

Quiescent cells generate energy from different energy-rich substrates, such as glucose, glutamine, and fatty acids through oxidative phosphorylation in the mitochondria. This is considered an energetically efficient mode of ATP production (DeBerardinis et al. 2008).

The metabolism of quickly proliferating cells (e.g. cancer cells) differs sharply from that of quiescent cells. Cancer cells need far more energy and nutrients than quiescent cells. In the early 1920's Otto Warburg pointed out that cancer cells have an altered metabolism compared to normal cells. Cancer cells upregulate glycolysis even under aerobic conditions and secrete lactate instead of oxidizing glucose completely to CO_2 via oxidative

phosphorylation. To commemorate the discovery of Warburg, this phenomenon was dubbed as Warburg effect or Warburg metabolism (Warburg, Wind, and Negelein 1927) (Figure 10). This modified metabolic state enables cancer cells to survive under unfavorable conditions such as inadequate oxygen supply (hypoxia), and to support rapid proliferation, progression and invasiveness.

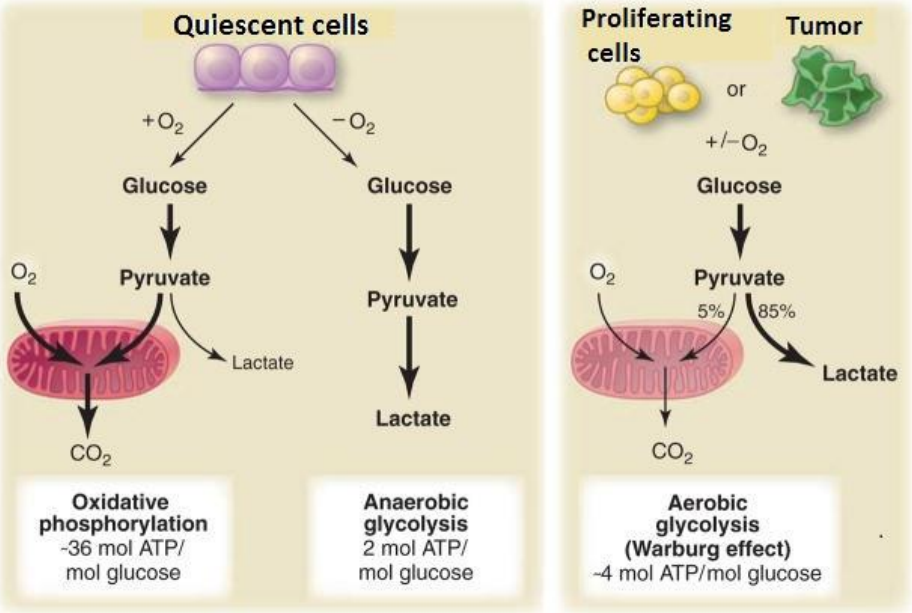

Figure 10. Differences between the metabolism of quiescent cells and proliferating cells
In Warburg effect cancer cells degrade the huge amount of glucose to lactate regardless the presence of O_2 that is often referred as aerobic glycolysis. Modified figure from (Vander Heiden, Cantley, and Thompson 2009).

In general, cells with Warburg metabolism can be characterized by their higher glycolytic rate, reduced pyruvate oxidation and enhanced lactate production. Moreover, cancer cells are often characterized by increased gluconeogenesis, glutaminolysis, elevated level of *de novo* fatty acid synthesis, reduced fatty acid oxidation, enhanced glycerol utilization, altered amino acid metabolism, and upregulated pentose phosphate shunt to provide building intermediates for nucleotide synthesis (Dakubo 2010).

3.2.10 Thermogenesis and AMPK

Historically, two types of adipose tissue were distinguished, the white adipose tissue (WAT) that stores triglycerides, and the brown adipose tissue (BAT) serving as a site for heat generation for non-shivering thermogenesis. Recently, a new type of adipose tissue was found that was termed beige adipose tissue (Wu et al. 2012; Petrovic et al. 2010). Beige cells reside in the WAT depots and while morphologically resemble white adipocytes, upon

adrenergic stimulation, beige cells can produce heat similarly to brown adipocytes (Petrovic et al. 2010; Kazak et al. 2015).

Brown adipose tissue (BAT) and beige adipose cells were highly specified on the adaptive thermogenesis where the mitochondrial uncoupling protein-1 (UCP1) has a prominent role. Beige cells are not only morphologically similar to white adipocytes but they also share the very low basal expression of UCP1. However, beige cells can upregulate UCP1 expression and enhance mitochondrial oxidation rate in response to cAMP or adrenergic stimulus similarly to brown adipocytes (Bartelt and Heeren 2014). Brown and beige adipocytes provide protection against hypothermia for small animals and newborn mammals. In mice BAT is located in the interscapular, cervical, axillary areas, while beige is found predominantly in the subcutaneous white fat depots. In humans BAT is located in the neck and interscapular region in newborns, while beige was identified in the suprascapulary area and around large blood vessels (Garruti and Ricquier 1992; Cannon and Nedergaard 2004).

During the differentiation of beige adipocytes SIRT1 has a major role via the deacetylation of peroxisome proliferator–activated receptor gamma (PPARγ) (Figure 11). AMPK was shown to be an upstream activator of SIRT1 (Canto et al. 2009), moreover, AMPK activation is involved in the differentiation of brown adipocytes (Canto et al. 2009) that together with the ability of AMPK to stimulate mitochondrial biogenesis made it likely that AMPK may have a role in regulating beige differentiation.

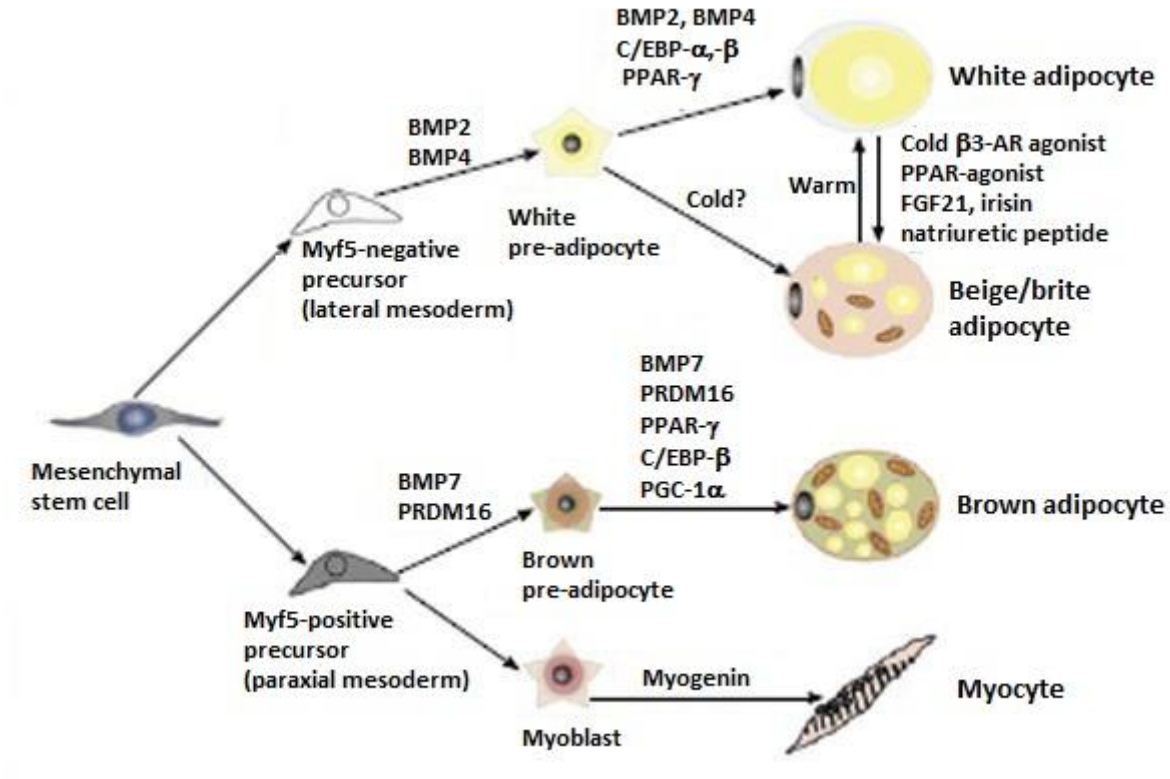

Figure 11. Development of white, brown and beige adipocytes

Previously white and brown adipocytes were hypothesized to be originating from a common precursor cell. It was pointed out that brown fat stems from the same progenitor cell ($Myf5^{+}$) as skeletal muscle. White adipocytes are derived from $Myf5^{-}$ progenitor cell. The $Myf5^{+}$ precursors are transformed into mature brown adipose cells by bone morphogenic protein 7 (BMP7), peroxisome proliferator–activated receptor-γ, CCAAT/enhancer binding protein (C/EBP) together with the transcriptional co-regulator PR domain-containing 16 (PRDM16) and PGC1α. White adipocytes can also be transformed to beige adipocytes upon cold exposure, a β-adrenergic agonist or a PPARγ agonist, fibroblast growth factor (FGF21), and peroxisome proliferator activated receptor gamma coactivator α (PGC1α). Modified figure form (Park, Kim, and Bae 2014).

4. AIMS

AMPK is a central actor in adaptation to energetic stress. We wanted to enlarge the current envelope of knowledge by studying the role of AMPK in reverting Warburg metabolism and better understanding its role in beige adipocyte differentiation.

We planned to answer the following questions.

- What is the metabolic effect of the joint application of AICAR and methotrexate (MTX)?
- What are the molecular actors in the metabolic rearrangements caused by the joint application of AICAR and MTX?
- Does the joint application of AICAR and methotrexate change cellular proliferation?
- What is the role of AMPK in the differentiation of beige adipocytes from human adipose–derived mesenchymal stem cells (hADMSCs)?

5. MATERIALS AND METHODS

5.1 Chemicals and reagents

All chemicals were from Sigma-Aldrich if not stated otherwise. For the pharmacological activation of AMPK, AICAR was used (Sigma-Aldrich or Santa Cruz Biotech).

5.2 Cell culture

4T1 - mouse mammary gland/breast tumor model. We received 4T1 cells from the Department of Biochemistry, University of Pécs, Pécs, Hungary. 4T1 cells were maintained in MEM (Sigma-Aldrich) supplemented with 10% heat-inactivated FBS (Sigma-Aldrich) and 2mM L-glutamine (Invitrogen), and 1% penicillin/streptomycin (Invitrogen) in humidified 5% CO_2 atmosphere at 37 °C.

hADMSC - human adipose-derived mesenchymal stem cells. hADMSCs were prepared from WAT of patients undergoing cardiac surgery (planned heart surgery, coronary bypass surgery, valve surgery, or Batista operation). Tissue samples were from the Department of Cardiology, University of Debrecen, Debrecen, Hungary. Cells were isolated from the pericardial adipose tissue. hADMSC cells were cultured in DMEM-F12 medium enriched with 10 % heat-inactivated FBS (Gibco) in humidified 5% CO_2 atmosphere at 37 °C.

MCF7 - human breast cancer cells. We received MCF7 cells from the Department of Immunology, University of Debrecen, Debrecen, Hungary. Cells were maintained in MEM (Sigma-Aldrich) supplemented with 10% heat-inactivated FBS (Sigma-Aldrich) and 2mM L-glutamine (Invitrogen), 1% penicillin/streptomycin (Invitrogen) in humidified 5% CO_2 atmosphere at 37 °C.

SAOS - human bone osteosarcoma cells. We received SAOS cells from the Department of Biophysics and Cell Biology, University of Debrecen, Debrecen, Hungary. Cells were maintained in low glucose DMEM (Sigma-Aldrich) supplemented with 10% heat-inactivated FBS (Sigma-Aldrich) and 2mM L-glutamine (Invitrogen), 1% penicillin/streptomycin (Invitrogen) in humidified 5% CO_2 atmosphere at 37 °C.

SKBR-3 - human mammary gland/breast cancer cells. We received cells from the Department of Biophysics and Cell Biology, University of Debrecen, Debrecen, Hungary. Cells were maintained in MEM (Sigma-Aldrich) supplemented with 10% heat-inactivated FBS (Sigma-Aldrich) and 2mM L-glutamine (Invitrogen), 1% penicillin/streptomycin (Invitrogen) in humidified 5% CO_2 atmosphere at 37 °C.

WM35 - human melanoma cells. We received WM35 cells from the Department of Biophysics, University of Debrecen, Debrecen, Hungary. Cells were maintained in RPMI-1640 medium (Sigma-Aldrich) supplemented with 10% heat-inactivated FBS (Sigma-Aldrich) and 2mM L-glutamine (Invitrogen), 0,5% penicillin/streptomycin (Invitrogen) in humidified 5% CO_2 atmosphere at 37 °C.

5.3 AICAR and MTX treatment schemes

Cells were treated with the pharmacological activator of AMPK, 5'-Aminoimidazole-4-carboxamide ribonucleotide (AICAR) and the antimetabolite methotrexate (MTX). 10 μM MTX and 100 μM AICAR and their combination 10 μM MTX+100 μM AICAR were applied in the subsequent experiments. In control samples we use PBS as vehicle. Cells were treated with the previously described drugs for 1 or 6 days.

5.4 Caspase assay

Caspase-3-like activity was measured by the cleavage of the fluorogenic tetrapeptide-amino-4-methylcoumarine conjugate (DEVD-AMC) as described by (Bai et al. 2001). Modifications were made as follows. At the end of treatment floating and adherent cells were pooled and resuspended in lysis buffer (10 mM HEPES, 0.1% w/v CHAPS, 5 mM DTT, 2 mM EDTA, 10 μg/ml aprotinin, 20 μg/ml leupeptin, 10 μg/ml pepstatin A, and 1 mM PMSF, pH=7.25). Cell lysates and substrates (50 μM) were combined in triplicates in caspase reaction buffer (100 mM HEPES, 10% sucrose, 5 mM DTT, 0.1% CHAPS, pH=7.25) at 37°C. Fluorescence of released AMC has been measured by a microplate fluorimeter (Thermo Labsystems Multiskan MS) at excitation wavelength of 380 nm and emission wavelength of 460 nm.

5.5 Cell cycle analysis

MCF7 cells were seeded in 6-well plate (10 000 cells/well). Cells were treated with 100 μM 5-Aminoimidazole-4-carboxamide 1-β-D-ribofuranoside (AICAR) and 10 μM methotrexate (MTX) and their combination for one or six days. For cell cycle analysis AICAR and/or methotrexate treated cells were fixed in ice-cold 70% EtOH for one hour and then stained with 50 μg/ml propidium iodide. 10 μL of PI staining solution to unstained cells. Mixed gently and incubated for 10 minute in the dark. Samples were measured on a FACS Calibur flow cytometer (Beckton Dickinson, Mountain View, CA,) at excitation wavelength of 535 nm and emission wavelength of 617 nm and the acquired data were processed with the BD CellQuest™ Pro. Software (Beckton Dickinson, Mountain View, CA).

5.6 Constructs, transfections

For silencing assay the pSuper RNAi system was used similarly as in (Bai et al. 2007).

To create a small hairpin RNA (shRNA)-expressing construct, double stranded DNA oligonucleotides were cloned into the pSuper vector. The oligonucleotides (containing the siRNA sequence) were annealed in annealing buffer (150 mM NaCl, 1 mM EDTA, 50 mM Hepes, pH=8.0).The resulting duplexes carried *Bgl*II and *Hin*dIII sites and were cloned into pSuper using these sites, resulting a ready to transfect mammalian expression vector that directs intracellular synthesis of shRNA-like transcripts. Transfections were performed each day throughout the six days of treatment using (siPGC1α1, siPGC1α2, siPGC1β, FOXO1, AMPKα1) constructs and polyethylenimine (PEI) as a transfection reagent. Sequences of oligonucleotides are listed in Table 1.

Table 1. Sequence of DNA oligonucleotides used to generate pSuper constructs

The interfering sequences are in bold.

*Bgl*II /sense/loop/antisense/T(5)/*Hin*dIII – Structure 1

*Hin*dIII/T(5)/antisense/loop/sense/*Bgl*II – Structure 2

Name	Sequence (5'-3')	Structure
siPGC1α-1 sense	GATCCCC**AAGACGGATTGCCCTCATTTG**TTCAAGAGA**CAAATGAGGGCAATCCGT**CTTTTTTTA	Structure 1
siPGC1α-1 antisense	AGCTTAAAAA**AAGACGGATTGCCCTCATTTGT**CTCTTGAA**CAAATGAGGGCAATCCGTCTT**GGG	Structure 2
siPGC1α-2 sense	GATCCCC**GACTATTGCCAGTCAAT**TAATTTCAAGAGA**ATTAATTGACTGGCAATAGTC**TTTTTA	Structure 1
siPGC1α-2 antisense	AGCTTAAAAA**GACTATTGCCAGTCAATTAAT**TCTCTTGAA**ATTAATTGACTGGCAATAGTC**GGG	Structure 2
siPGC1β sense	GATCCCC**AGCAACTCTATGCTGACTTTC**TTCAAGAGA**GAAAGTCAGCATAGAGTTGC**TTTTTTA	Structure 1
siPGC1β antisense	AGCTTAAAAA**AGCAACTCTATGCTGACTTTC**TCTCTT**GAAGAAAGTCAGCATAGAGTTGC**TGGG	Structure 2
FOXO1 sense	GATCCCCCAGG**ACAATAAGTCGAGTTAT**TTCAAGAGA**ATAACTCGACTTATTGTCCTG**TTTTTA	Structure 1
FOXO1 antisense	AGCTTAAAAAC**AGGACAATAAGTCGAGTTAT**TCTCTTGAA**ATAACTCGACTTATTGTCCTG**GGG	Structure 2
AMPKα1 sense	ATCCCC**GTTGCCTACCATCTCATAATA**TTCAAGAGA**TATTATGAGATGGTAGGCAAC**TTTTTA	Structure 1
AMPKα1 antisense	AGCTTAAAAA**GTTGCCTACCATCTCATAATA**TCTCTTGAA**TATTATGAGATGGTAGGCAAC**GGG	Structure 2

5.7 Isolation, culture and differentiation of human adipose derived mesenchymal stem cells (hADMSCs)

Tissue samples were collected and processed on the day of the heart surgery. Adipose tissues were disentangled from fibrous parts and blood vessels, minced into small pieces and remaining tissue parts were digested in PBS with 120 U/ml collagenase for 1 hour at 37 °C with gentle agitation. The separated tissue was filtered through at a 100 μM pore size sieve to remove the unnecessary tissue parts. The cell suspension was centrifuged for 10 min at 1300 rpm and the pellet of stromal cells (hADMSCs) was resuspended in DMEM-F12 medium containing 10% FBS (Gibco) and seeded to the appropriate plate. After the cells reached confluency, differentiation was started. When cell culture reached confluency differentiation was started. For white adipogenic differentiation cells were treated as in Fischer-Posovszky and co-workers protocol (Fischer-Posovszky et al. 2008). DMEM-F12 supplemented with 2μmol/l rosiglitazone, 25 nmol/l dexamethasone, 0.5 mmol/l methyliso-buthylxantine, 0.1 μmol/l cortisol, 0.01 mg/ml transferrin, 0.2 nmol/l triiodotyronin, and 20 nmol/l human insulin).

After 4 days, medium was changed, and cells are further cultured in DMEM/F12 supplemented with 0.1 μmol/l cortisol, 0.01 mg/ml transferrin, 0.2 nmol/l triiodotyronin, and 20 nmol/l human insulin. Within a few days, the cells start to accumulate lipids, and small lipid droplets are visible after approximately 1 week. For brown adipogenic differentiation cells were treated as in Elabd and co-workers protocol (Elabd et al. 2009). Cells were maintained in DMEM/Ham's F12 media supplemented with 10 μg/ml of transferrin, 0.85 μM insulin, 0.2 nM triiodothyronine, 1 μM dexamethasone (DEX), and 500 μM isobutyl methylxanthine (IBMX). After 3 days, the medium was changed (DEX and isobutyl methylxanthine excluded) and various amounts of rosiglitazone were added for the indicated periods. Media were then changed every other day, and cells were used at the indicated days. 100 μM AICAR was applied to white adipocytes differentiation medium to activate AMPK. During the differentiation FBS free medium was used. Cells were differentiated for 14 days.

5.8 Sulforhodamine B assay

Growth inhibition was detected using sulforhodamine B (SRB) assay that measures changes in total protein content. Cells were seeded into a 96-well plate (3000–5000 cells/well). Cells were grown in the presence of vehicle and treated with AICAR, MTX, AICAR+MTX at one and six days. At the end of the treatment, after fixation in situ by 50% trichloroacetic acid (TCAA) cells were stained with sulforhodamine B (SRB) solution (0.4% in 1% acetic acid). Unbound dye was removed by washing with 1% acetic acid. Bound stain was solubilized with 10 mM TRIS base. Absorbance was read on an automated plate reader (Thermo Labsystems Multiskan MS) at 540 nm.

5.9 Measurement of mitochondrial membrane potential

Mitochondrial membrane potential was determined by DioC6 (3,3-dihexyloxacarbocyanine iodide) staining. Cells were seeded into a 96-well plate (25, 000 cells/well). After one- and six-day treatment, cells were harvested by adding trypsin/EDTA, and the detached cells were stained with 40 nM DioC6 for 30 min), then subsequently washed with phosphate-buffered saline (PBS). Cells were subjected to flow cytometric analysis (FACSCalibur, BD Biosciences) with 20,000 events collected for each sample; each measurement point was repeated in 3 parallel replicates. Control cells were treated with 10 μM Carbonyl cyanide 4-(trifluoromethoxy)phenylhydrazone (FCCP) to dissipate mitochondrial membrane potential. The value measured in the FCCP-treated cells were subtracted from all groups. The FCCP-corrected values were displayed and were used for statistical analysis.

5.10 Measurement of superoxide production

Superoxide was measured using hydroethidine (HE) staining. Cells were prepared similarly to mitochondrial membrane potential measurement and were stained by 2 mM HE for 30min. Fluorescence was analyzed by flow cytometry (FACSCalibur, BD Biosciences). Superoxide production was indicated as a mean of HE fluorescence in each sample. Cells were subjected to flow cytometric analysis with 20,000 events collected for each sample, each measurement point was repeated in 3 parallel replicates.

5.11 Oxygen consumption

Oxygen consumption was measured using an XF96 oximeter (Seahorse Biosciences, North Billerica, MA, USA). Cells were seeded in 96-well XF 96 assay plates (~2000 cell/well) and were treated as described before. Oxygen consumption rate (OCR, reflecting mitochondrial oxidation) and changes in pH, extracellular acidification rate (ECAR, reflecting glycolysis) were recorded every 30 min to follow the transfection effects. Cells were treated with etomoxir (50 μM), then oligomycin (10 μM) and finally, antimycin (10 μM). Data were normalized to protein content and normalized readings were used for calculations. OCR values after antimycin treatment were subtracted from all other values. We named the readings for the untreated cells *baseline OCR*. OCR after etomoxir treatment represents the oxygen consumption related to glucose and amino acid oxidation (*Glc+AA*), while the difference between baseline and Glc+AA OCR represents fatty acid oxidation (*FAO*). The oligomycin-resistant respiration gives information on the leakage through the inner membrane of the mitochondria (*proton leak*). Data were normalized to protein content and normalized readings were displayed.

In the case of adipocytes cells were seeded and also differentiated in 96-well XF96 well assay plates. After differentiation the baseline oxygen consumption was rerecorded,

subsequently cells were given a bolus dose of dibutryil-cAMP (500 μM final concentration) mimicking an adrenergic stimulation. Then the oxygen consumption was recorded every 30 minutes and the last reading took place at 7 hours post-treatment. Finally, a single bolus dose of antimycin A (10 μM) was given to the cells for baseline correction. In both case data were normalized to protein content and normalized readings were evaluated.

5.12 RNA isolation, reverse transcription and QPCR

Total RNA was prepared using TRIzol reagent (Invitrogen) according to the manufacturer's instructions. Two micrograms of RNA were used for reverse transcription (High Capacity cDNA Reverse Transcription Kit, Applied Biosystems, Foster City, CA, USA). Diluted cDNA was used for reverse transcription-coupled quantitative PCR (RT-qPCR). The qPCR reactions were performed with the qPCRBIO SyGreen Lo-ROX Supermix (PCR Biosystems) except for TBX1 where the primer and probes were designed and supplied by Applied Biosystems (Taqman Hs00271949_m1, Applied Biosystem) using a Light-Cycler 480 system (Roche Applied Science) for detection. Gene expression was normalized to the geometric mean of human 36B4, 18S, and cyclophyllin and G6PD values. Gene expression values were calculated based on the ΔΔCt method, where white adipose sample were designated as calibrator. Primers are listed in Table 2.

Table 2. List of primers used in the study

ACO2 (human)	F: CCA GAG ACC GAC TAC CTG ACG R: CCA CTT GTC AAA AGG CTC CAG
Actin (human)	F: GAC CCA GAT CAT GTT TGA GAC C R: CAT CAC GAT GCC AGT GGT AC
AMPK (human)	F: CAT GAA GAG GGC CAC AAT CAA R: GCC AAA GGA TCC TGG TGA TTT
ATP5G1 (human)	F: CTAAACAGCCTTCCTACAGCAACTT R: TGAACCAGCCACACCAACTGT
ATP5G1 (murine)	F: GCT GCT TGA GAG ATG GGT TC R: AGT TGG TGT GGC ATC A
Cyclophilin A (human)	F: GTCTCCTTTGAGCTGTTTGCAGAC R: CTTGCCACCAGTGCCATTAT
Cyclophilin A (murine)	F: TGG AGA GCA CCA AGA CAG ACA R: TGC CGG AGT CGA CAA TGAT
FOXO1 (human)	F: GTTCATTGAGCGCTTAGACTG R: AAGTGTAACCTGCTCACTAACCC
FOXO1 (murine)	F: AAG GAT AAG GGC GAC AGC AA R: TCC ACC AAG AAC TCT TTC CA
Fumarase (human)	F: CTCGTTTTGGCCTCCGAACG R: TAACTGGGGTTGGCATGCGT
Fumarase (murine)	F: CGC AGG TCA TCA AAA TTG GGC G R: GGG CAG TGA CAA AAG GCA AAC C
GAPDH (human)	F: CGTATTGGGCGCCTGGTC R: GGAATTTGCCATGGGTGGAA
GAPDH (murine)	F: CAA GGT CAT CCA TGA CAA CTT TG

	R: GGC CAT CCA CAG TCT TCT GG
IDH2 (human)	F: GGTGGAGATGGATGGTGATGA R: GTGATGGTGGCACACTTGACT
IDH2 (murine)	F: CGC CAT TAC CGA GAA CAC CAG A R: GTG GTG TTC AGG AAG TGC TCG T
18s (human)	F: TCGAGGCCCTGTAATTGGAAT R: TCCCAAGATCCAACTACGAGC TT
18s (murine)	F: GGGAGCCTGAGAAACGGC R: GGGTCGGGAGTGGGTAATTTT
36B4 (human)	F: CCATTGAAATCCTGAGTGATGTG R: GTCGAACACCTGCTGGATGAC
36B4 (murine)	F: AGA TTC GGG ATA TGC TGT TGG R: AAA GCC TGG AAG AAG GAG GTC
PGC1α (human)	F. AGAATTGGCTTATGGATGTACAGG R: TTTGTTGATCATTTCCAGCAATAAT
PGC1α (murine)	F: AAGTGTGGAACTCTCTGGAACTG R: GGGTTATCTTGGTTGGCTTTATG
PGC1-β (human)	F: GTGCTGACAAGAAATAGGAGAGG R: CTCTTCTGAATTGGAATCGTAGTC
PGC1-β (murine)	F: TGGAGACTGCTCTGGAAGGT R: TGCTGCTGTCCTCAAATACG
UCP1 (human)	F: AACGAAGGACCAACGGCTTTC R: GGCACAGTCCATAGTCTGCCTTG
UCP1 (murine)	F: CTTTGCCTCACTCAGGATTGG R: ACTGCCACACCTCCAGTCATT
UCP2 (human)	F: CTACAAGACCATTGCCCGGAG R: ACAATGGCATTACGAGCAACA
UCP2 (murine)	F: TGGCAGGTAGCACCACAGG R: CATCTGGTCTTGCAGCAACTCT
NDUFA2 (human)	F: CGATATTAACAAGGATGGCGG R: TCTCAATGAAGTCCCTGACGC
NDUFA3 (human)	F: AGACAAAGATGGCTGCGAGAG R: CGTGGCCTTGTTGATCATGAC
NDUFB5 (human)	F: GTATTCATTGGTCAAGCTGAACTAG R: CAGCTCCTTTACCCGTAATTCAGC
COX17 (human)	F: GATGCGTGTATCATCGAGAAAG R: CAGCAGACCACCATTTCATATTT
CPT1A (human)	F: CAGGCGAGAACACGATCTTC R: GCGGATGTGGTTTCCAAAG
CPT2 (human)	F: CCAGGCTGCCTATTCCCAAAC R: AGGGTCCCGAAATGTAGCTTG
MCAD (human)	F: AGAATTGGCTTATGGATGTACAGG R: TTTGTTGATCATTTCCAGCAATAAT
ME2 (human)	F: TGTTAAGGCTGTTGTAGTGACTGA R: TAAGAGTGCGATATTATCAGTTCCC
MLYCD (human)	F: AACATCCAGGCAATCGTGAAG R: GAGGAAACTCTCTCTGCAACTCC
PKLR (human)	F: CACCAAGAACCCCAGAACTCC R: GGAATAAGGGAAAGGCCCAAG
CAT (human)	F: TGAAAATTTGTGCATCCTTCA R: ATTCTGGAGAAGTGCGGAGA
SOD1 (human)	F:CCCACCGTGTTTTATGGATA R:AGGTGTGGGGAAGCATTAAA

SOD2 (human)	F:AATCAGGATCCACTGCAAGG R:TAAGCGTGCTCCCACACAT
SDHB (human)	F: CCTTCGGGTGCAAGCTAGAGT R: CAAGGCTGGAGACAAACCTCA
CIDEA (human)	F: TCTCCAACCATGACAGGAGCAG R: AATGCGTGTTGTCTCCCAAGGT
PRDM16 (human)	F: CACTGTGCAGGCAGGCTAAGAA R: AGAGGTGGTTGATGGGGTGAAA
TMEM26 (human)	F: ACCTCCCATGTGTGGACATCCT R: ACCAACAGCACCAACAACCTCA
G6PD (human)	F: GCCTCATCCTGGACGTCTTCT R: GGTGCCCTCATACTGGAAACC

5.13 SDS-PAGE and Western Blotting

Cells were lysed in RIPA buffer (50 mM Tris, 150 mM NaCl, 10% SDS, 1% Nonidet P-40, 1 mM Na_3VO_3, 1 mM NaF, 0.5% sodium deoxycholate, 1 mM phenylmethylsulfonyl fluoride, protease inhibitor mixture, pH=8.0). Proteins were separated by sodium dodecyl sulfate-polyacrylamide gel electrophoresis (SDS-PAGE) on 8% acrylamide gels and blotted onto nitrocellulose membranes. After blocking in 5% (w/v) non-fat dry milk, the membranes were washed with 1x TW-TBS. Membranes were probed with primary antibodies (see Table 3.). Monoclonal acetyl-CoA carboxylase (ACC) and polyclonal phospho-acetyl-CoA-carboxylase antibody (pACC) and polyclonal AMPKα and polyclonal phospho- AMPKα antibodies were applied overnight, at 4 C˚, whereas monoclonal Anti-β-Actin –Peroxidase antibody for 1 hour at room temperature.

Table 3. List of the primary antibodies used in the current study

Target	Company	Dilution
acetyl-CoA carboxylase (ACC), rabbit anti-human monoclonal antibody	Cell Signaling, Danvers MA, USA	1:1000
phospho-acetyl-CoA carboxylase (pACC), rabbit anti-human polyclonal antibody	Cell Signaling, Danvers MA, USA	1:500
AMPKα rabbit anti-human polyclonal antibody	Sigma-Aldrich	1:500
phospho-AMPKα (pAMPKα), rabbit anti-human polyclonal antibody	Cell Signaling, Danvers MA, USA	1:1000
anti-β-actin peroxidase-coupled antibody	Sigma-Aldrich	1:20000

As the secondary antibody we used an IgG peroxidase HRP conjugate (Sigma-Alrdich, 1:2000). Bands were visualized by enhanced chemiluminescence reaction (West Pico ECL Kit, Thermo Scientific, Walthman, Massachusetts, USA).

5.14 Database screening

The effect of AMPKα1, FOXO1 and PGC1α expression on breast cancer, survival was assessed through the Kaplan-Meier plotter database (http://kmplot.com/analysis/) including those patients, where ER status was derived from gene expression data. Overall survival was analyzed.

5.15 Statistical analysis

Significance was analyzed by Student's *t*-test, for multiple comparisons ANOVA test was applied. Error bars represent ± S.D., unless noted otherwise.

6. RESULTS

6.1 AMPK in Warburg

6.1.1 Combined treatment of AICAR and MTX inhibits MCF-7 proliferation, lowering proliferation rate

As the first step of the study, we determined the sensitivity of MCF-7 cells (a cellular model of invasive ductal breast carcinoma) to AICAR and MTX. Cells were treated with MTX (3–300 μM), or AICAR (100–1000 μM) or the combination of the two reagents (Figure 12A).

The rate of cell proliferation was estimated through an inverted microscope and on the sixth day of the assay total protein content - that corresponds to cell number - was assessed using SRB assay. When cells were treated with MTX or AICAR individually, we did not detect decreases in total protein content, however, the combination of AICAR and MTX resulted in a marked decrease of total protein (Figure 12A). On day six, 10 μM MTX + 100 μM AICAR combination (abbreviated as AICAR+MTX) resulted in 50% reduction in cell numbers; these AICAR and MTX concentrations were used in the subsequent experiments.

As next step we performed a time course experiment (Figure 12B). The efficiency of AICAR+MTX combination became evident on the third day of treatment and turned statistically significant on day six. To measure the dynamics of biochemical changes we carried out all measurements at an early time point (1 day post treatment, short treatment) and late time point (6 days post treatment, prolonged treatment).

An obvious explanation for reduced total protein upon AICAR+MTX treatment could be cell death. Importantly, we did not detect major increase in PI positive cells neither on day 1, nor on day 6 (Figure 12C) or increases in caspase activity (data not shown), suggesting that increased cell death is not the cause of reduced cell numbers, it is due to the slowdown of proliferation.

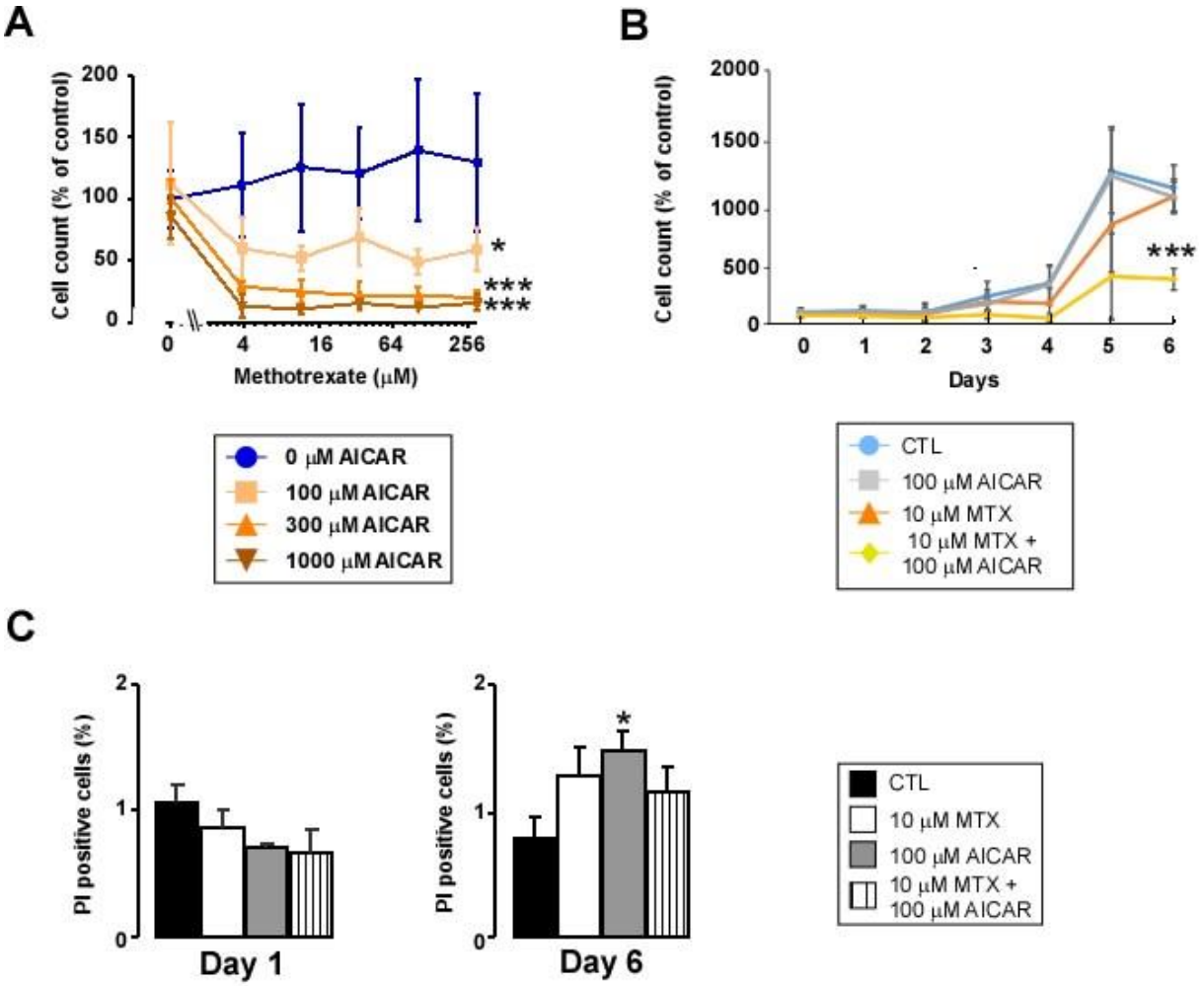

Figure 12. Combined treatment with AICAR and MTX decreases MCF-7 proliferation.

(A) MCF-7 cells were seeded on 96-well culture plate at 3000–4000 cells/well and were treated with MTX and AICAR as indicated (n=4 for each measurement point). After 6 days in culture total protein was determined using SRB assay. A typical experimental result is shown. **(B)** MCF-7 cells were seeded on 96-well culture plate at 3000–4000 cells/well and were treated with MTX and AICAR as indicated (n=4 for each measurement point). Seven parallel plates were made and started on the same day. Each day a plate was fixed and at the end of the experiment total protein was determined using SRB in all plates. The measurement point day 0 represent the total protein before the beginning of treatment. A typical experimental result is shown. **(C)** MCF-7 cells were seeded on 6-well culture plate at 90 000–100 000 cells/well. Cells were treated with 100 μM AICAR and 10 μM MTX for 1 and 6 days (n=3 for each measurement point). Dead cells were stained using propidium iodide, cells were harvested by trypsinization and were analyzed on a FacsCalibur flow cytometer. A typical experimental result is shown. * and *** indicate statistically significant difference between control and treated cells at $p < 0.05$ and $p < 0.001$, respectively.

6.1.2 The joint application of AICAR and MTX induces AMPK reverts Warburg metabolism

We followed up the lead of cell proliferation slowdown and we hypothesized an anti-Warburg rearrangement of metabolism.

In the first place we tested whether AICAR indeed activates AMPK by monitoring the phosphorylation of acetyl-CoA carboxylase (pACC). On day 1, similarly to the results on proliferation (Figure 12C), AICAR did not induce AMPK individually, only when applied in combination with MTX. At prolonged treatment, on day 6, MTX, AICAR and MTX+AICAR robustly induced AMPK (Figure 13).

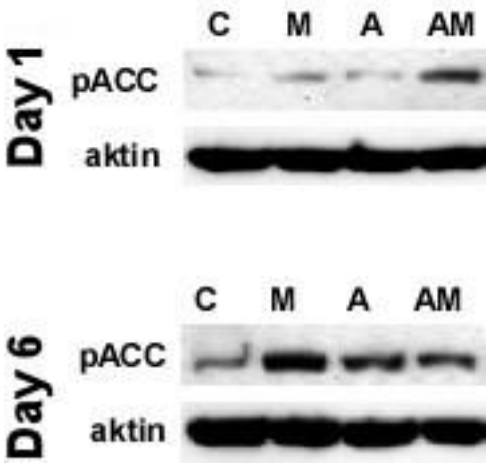

Figure 13. AMPK activation upon AICAR+MTX treatment.

Activation of AMPK was determined by Western blot analysis of acetyl-CoA carboxylase phosphorylation (pACC) on day 1 and day 6. Actin was used as loading control.

C: control; M: MTX; A: AICAR; AM: AICAR+MTX. A typical experimental result is shown.

AMPK activation was translated into mitochondrial activation indicated by higher DioC6 fluorescence indicating increases in mitochondrial membrane potential (Figure 14).

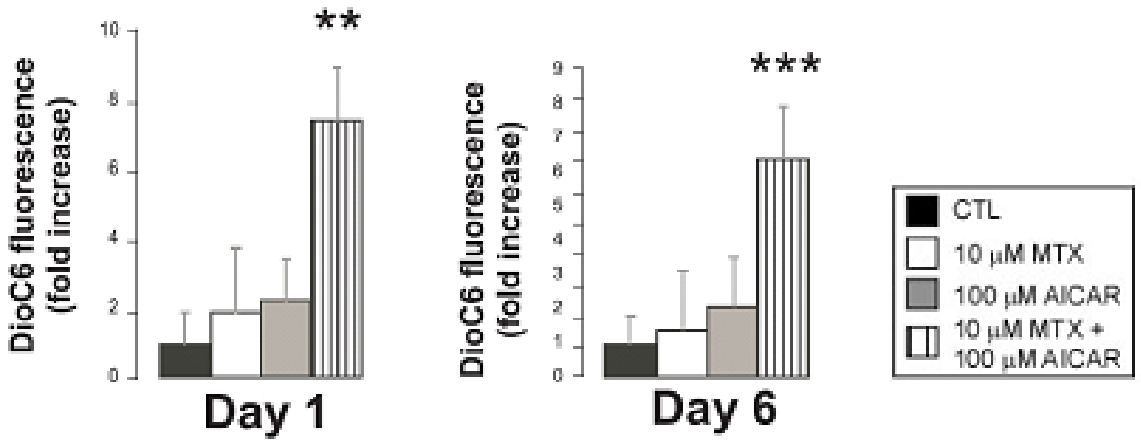

Figure 14. Activation of mitochondrial oxidation upon treatment with AICAR + MTX

Mitochondrial membrane potential was measured by DiOC6 staining. MCF-7 cells were seeded in 96-well culture plate at 25,000 cells/well and were treated with MTX and/or AICAR as indicated (n=4 for each measurement point). On day 1 and day 6 cell were loaded with DioC6, cells were harvested by trypsinization and were analyzed on a FacsCalibur flow cytometer. Mean of fluorescence intensity of 4 parallel samples were averaged and depicted. A typical experimental result is shown.

We continued our research with the measurements of the major metabolic regulator and effector genes. At Day 1 we observed the induction of peroxisome proliferator activated receptor gamma coactivator (PGC)-1α and forkhead transcription factor-1 (FOXO1) upon AICAR+MTX treatment (Figure 15). In line with these, the expression of ATP5g1, a subunit of ATP synthase and isocitrate dehydrogenase-2 (IDH2), a marker of tricarboxylic acid (TCA) cycle (Figure 15) were induced slightly, suggesting that higher expression of PGC1α and FOXO1 was translated into gene expression programs supporting mitochondrial activity. The expression of PGC1α and FOXO1 further enhanced by Day 6, furthermore, PGC1β, another key mitotropic regulator (Lai et al. 2008; Uldry et al. 2006; Wareski et al. 2009) boosted upon AICAR+MTX treatment (Figure 15). Consequently, at Day 6 enhanced expression of ATP5g1 and IDH2 in the AICAR+MTX treated cells was exacerbated, furthermore, other TCA cycle enzymes expression level, fumarase and aconitase-2 (ACO2) were also elevated (Figure 15).

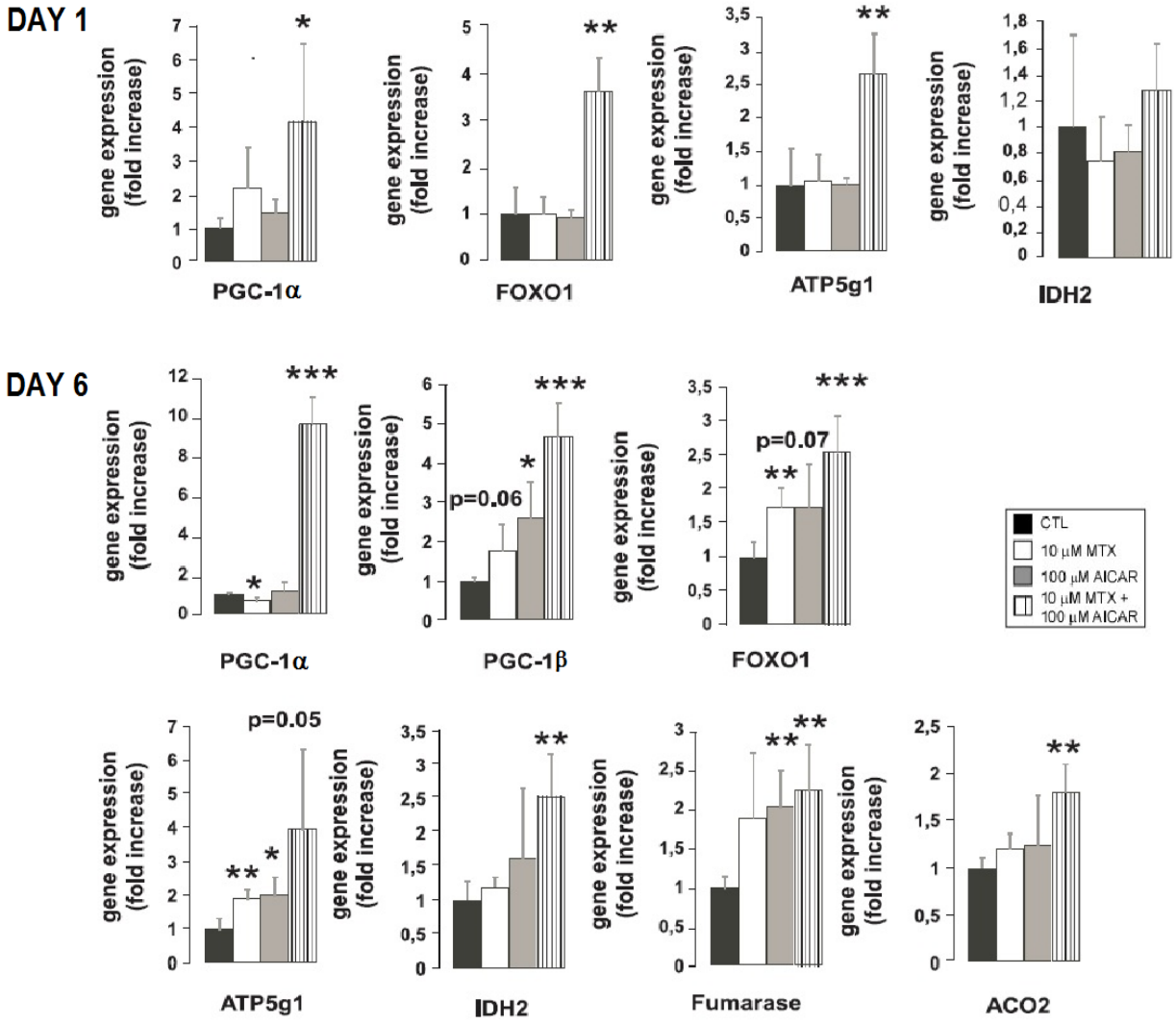

Figure 15. Activation of mitochondrial oxidation upon treatment with AICAR + MTX.

The expression of a set of genes were analyzed using RT-qPCR on DAY 1 and on DAY 6 in MCF-7 cells treated with MTX and/or AICAR (n=4/4/4/4) as indicated. Bars represent fold changes relative to control samples. All gene abbreviations are listed in the text. A typical experimental result is shown. *, ** and *** indicate statistically significant difference between control and treated cells at $p < 0.05$, $p < 0.01$ and $p < 0.001$, respectively.

As it was shown, anti-Warburg rearrangement of metabolism leads to the suppression of glycolysis (Wallace 2012). To follow up, we tried to compare the rate of glycolysis and mitochondrial oxygen consumption by using the Seahorse XF96 instrument. Surprisingly, on day 1 in AICAR+MTX treated cells glycolysis was induced (Figure 16), evidenced by decreases in the ratio of oxygen consumption rate (OCR) / extracellular acidification rate (ECAR). In contrast to that, on day 6 OCR/ECAR ratio increased in AICAR+MTX pointing out increased mitochondrial activity and lower dependence of cells on glycolysis (Figure 16).

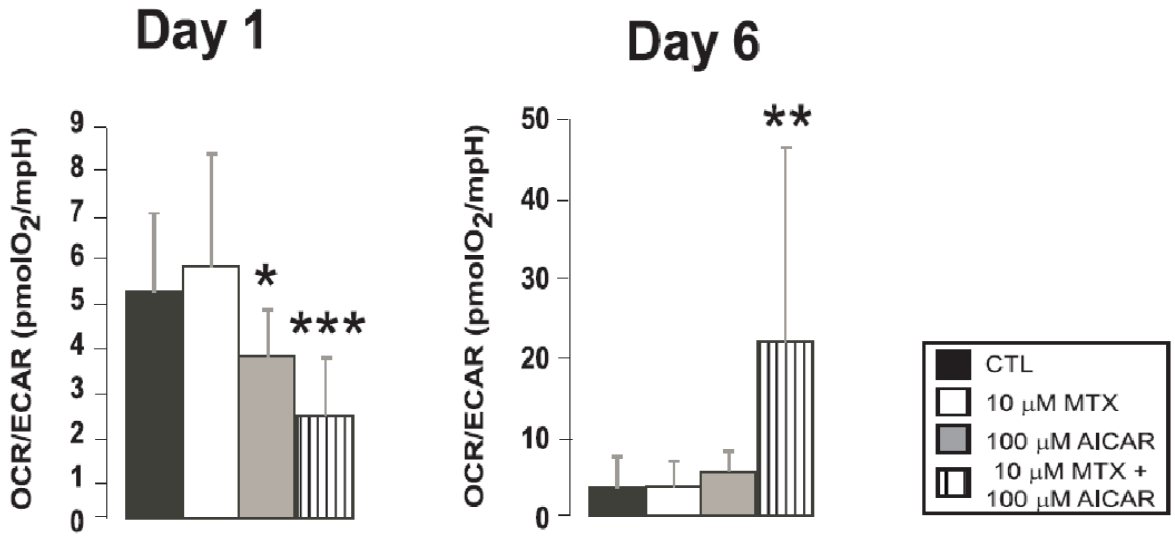

Figure 16. Changes in the ratio of glycolysis and mitochondrial oxidation upon treatment with AICAR + MTX.

The rate of mitochondrial oxygen consumption and glycolysis were assayed by Seahorse XF96 analyzer on day 1 and day 6 as described in the Materials and Methods section (n = 23/23/23/23). The OCR/ECAR ratio reflecting the ratio of mitochondrial oxidation and glycolytic flux is shown. OCR-oxygen consumption rate; ECAR-extracellular acidification rate. A representative result is shown. *, ** and *** indicate statistically significant difference between control and treated cells at $p < 0.05$, $p < 0.01$ and $p < 0.001$, respectively.

Taken together treating MCF-7 cells with AICAR+MTX at early time point (i.e. day 1) moderately induces mitochondrial metabolism, but supports glycolysis - paradoxically bringing about rather pro - Warburg changes. However, prolonged (i.e. day 6) AICAR+MTX treatment largely induces mitochondrial oxidation and suppresses glycolysis setting off true anti-Warburg changes.

6.1.3 AICAR+MTX treatment leads to G1/S and G2/M blockade

G1/S transition is under metabolic control: if cells do not possess the necessary substrates for successful replication, the G1 to S transition of the cell cycle is blocked (Colombo et al. 2011). Our preliminary data suggested an anti-Warburg rearrangement of cellular metabolism upon AICAR+MTX treatment, therefore we set out to analyze changes in cell cycle. Short term AICAR+MTX treatment (day 1) reduced the number of cells in S and slightly elevated the number of cells in G2 (Figure 17). When we checked the ratios between different cell cycle phases, it was apparent that G1/S and G2/S ratios increased, while G1/G2 ratio remained constant suggesting G2/M and probably G1/S block. Prolonged AICAR+MTX treatment (day 6) showed similar changes, elevated proportion of G2 cells with decreased

number of cells in S phase (Figure 17) and increases in the proportions of cells in G1 and G2 as compared to the number of cells in S-signs of simultaneous G1/S and G2/M block in the cell cycle.

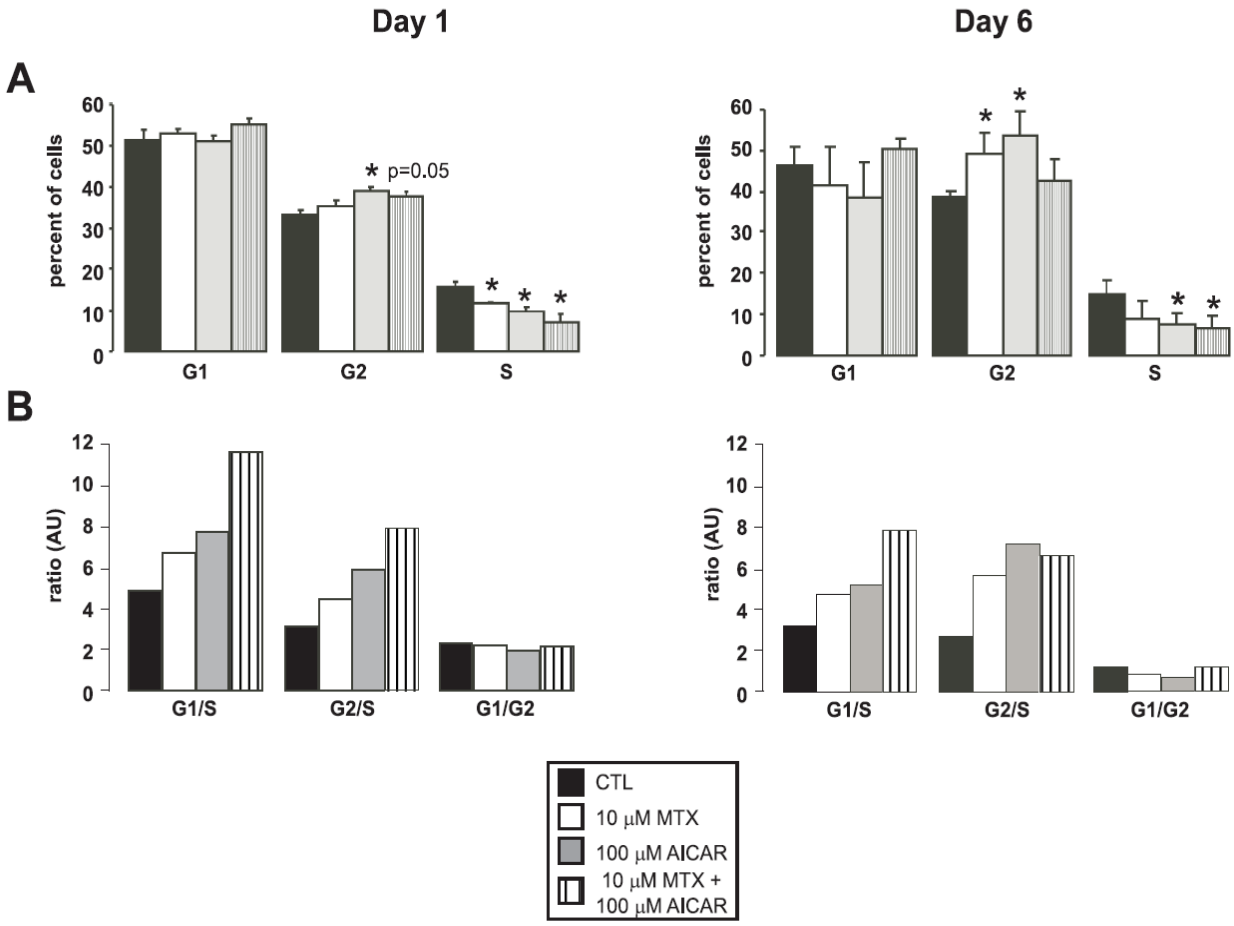

Figure 17. AICAR+MTX treatment blocks the cell cycle

(A) MCF-7 cells were seeded in 6-well plates at 10,000 cells/well (n=6/6/6/6). Cells were treated with AICAR and/or MTX for the time indicated. Cells were fixed, permeabilized and charged with propidium iodide. DNA content was analyzed by flow cytometry. The data on day 1 is the average of 3 parallel experiments, while the data for day 6 is the average of 2 parallel experiments. (B) The data on panel A was further analyzed and the ratio between the different stages were calculated and depicted. The data derived from fig 5A. * indicate statistically significant difference between control and treated cells at $p < 0.05$.

6.1.4 Combined treatment of SKBR-3 and 4T1 cells with AICAR and MTX reduces cell proliferation rate in an additive fashion

All previous data were obtained on one cell line (MCF7), therefore we verified our findings on two other breast cancer cell lines. The human SKBR-3 and the murine 4T1. SKBR-3 cells, similarly to MCF-7, were not sensitive to MTX and AICAR when administered alone. Meanwhile the AICAR+MTX combination slowed down cellular proliferation (Figure 18A) that coincided with increases in the expression of several markers of mitochondrial oxidation (FOXO1, PGC1α, PGC1β, fumarase, IDH2 and ACO2) that are the same as in the case of

MCF-7 (Figure 18B). 4T1 cells were very sensitive to MTX, roughly thousand fold, less MTX was already antiproliferative in 4T1 cells as compared to MCF-7 or SKBR-3 (Figure 18C). Despite the changes in sensitivity we did observe a slightly enhanced antiproliferative effect of the 300 μM AICAR + 7.8 nM MTX or 300 μM AICAR + 15.6 nM MTX combination as compared to the individual components alone (Figure 18C). Similar to our results with MCF-7 and SKBR-3 cells, 300 μM AICAR + 7.8 nM MTX treatment induced slightly the expression of FOXO1, ATP5g1, fumarase and IDH2 in 4T1 cells (Figure 18D). Taken together, the additive effect of AICAR+MTX treatment is not specific for MCF-7 but it acts similarly in other breast cancer cell lines as well. In order to determine the specificity of AICAR+MTX treatment we tested two other cell lines, WM35 that is a model for melanoma and SAOS that is a model for osteosarcoma; none of them was susceptible to the MTX+AICAR combination (data not shown).

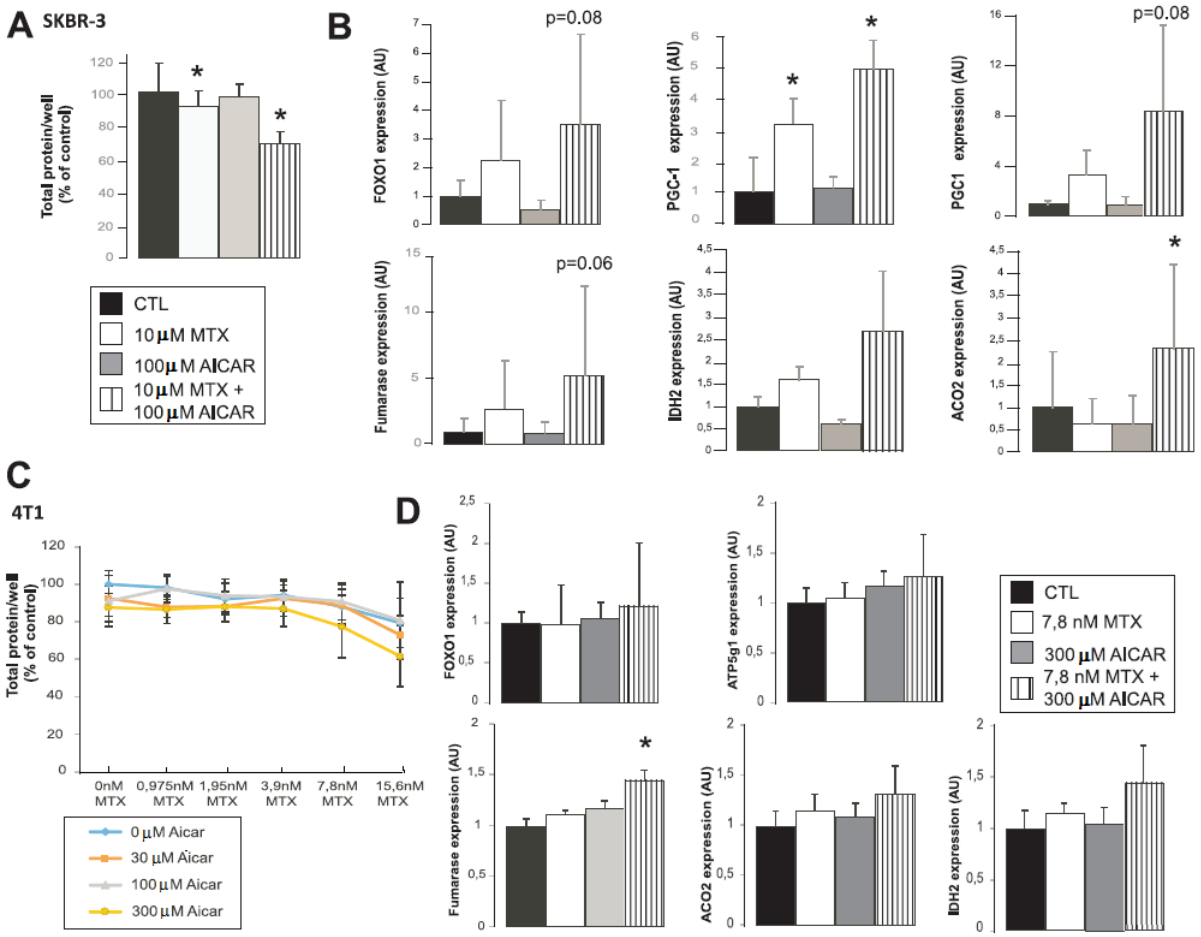

Figure 18. Combined treatment of SKBR-3 and 4T1 cells with AICAR and MTX reduces cell proliferation rate in an additive fashion

(A) SKBR-3 cells were seeded on 96-well culture plate at 3000–4000 cells/well and were treated with MTX and AICAR as indicated (n=4 for each measurement point). After 3 days in culture total protein was determined using SRB assay. The data is the average of 3 parallel experiments. **(B)** The expression of a set of genes was analyzed using RT-qPCR on day 3 in SKBR-3 cells treated with MTX and/or AICAR (n=6/6/6/6) as indicated. Bars represent fold changes relative to control samples. All gene abbreviations are listed in the text. A typical experimental result is shown. **(C)** 4T1 cells were seeded on 96-well culture plate at 3000–4000 cells/well and were treated with MTX and AICAR as indicated (n=4 for each measurement point). After 2 days in culture total protein was determined using sulforhodamine B. The figure shows the average of 3 parallel experiments. **(D)** The expression of a set of genes was analyzed using RT-qPCR on day 2 in 4T1 cells treated with MTX and/or AICAR (n=6/6/6/6) as indicated. Bars represent fold changes relative to control samples. All gene abbreviations are listed in the text. A typical experimental result is shown. * indicate statistically significant difference between control and treated cells at $p < 0.05$.

6.1.5 The inhibitory properties of the AICAR+MTX treatment can be reverted by silencing of mitotropic transcription factors

AICAR+MTX treatment brought about anti-Warburg alterations in metabolism and led to G1/S and G2/M block in cell cycle. Enhanced expression of PGC1α, PGC1β and FOXO1 (Figure 15C) correlates with enhanced mitochondrial activity and the slowdown of proliferation suggests a central role for these proteins in the antiproliferative effect of the AICAR+MTX treatment. We prepared shRNA expressing constructs (siPGC1α1, siPGC1α2, siPGC1β, FOXO1, AMPKα1) targeting these proteins in order to assess their possible role. Both short (until day 1) and long term (until day 6) silencing (transfection each day) efficiently reduced the expression of target mRNA (Figure 19A). When these constructs were transfected into MCF-7 cells the proliferation of the cells doubled (Figure 19B). Furthermore, reduced cell proliferation upon AICAR+MTX treatment was abolished by the end of the 6-day treatment (Figure 19B).

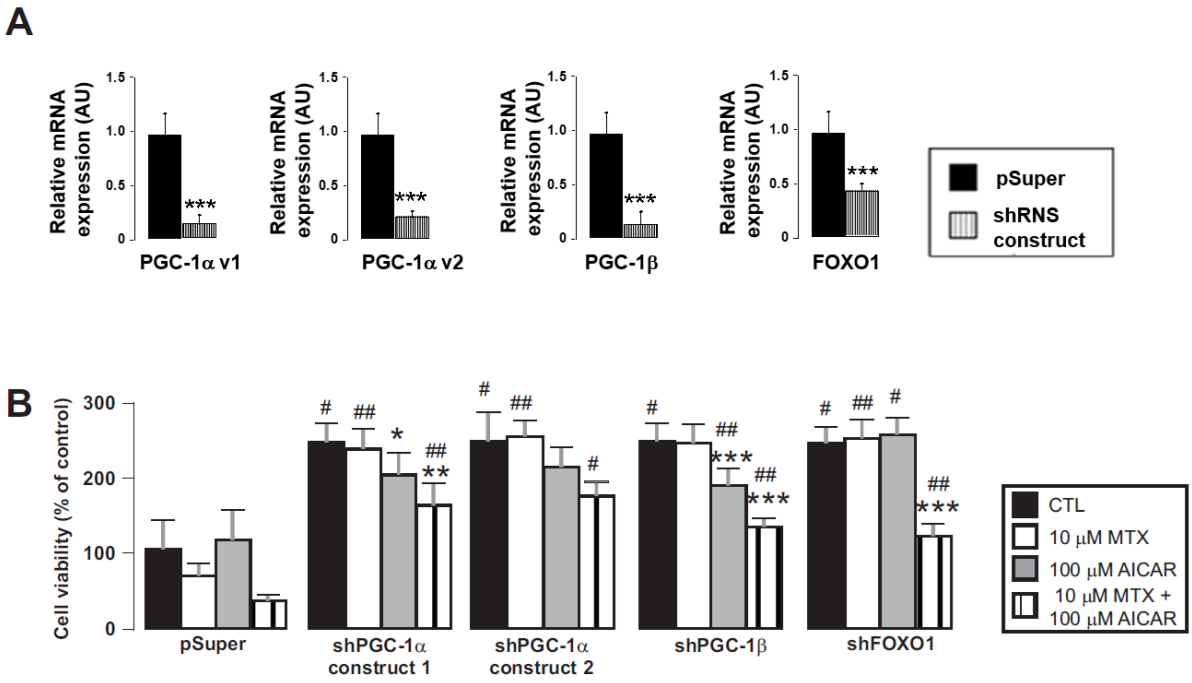

Figure 19. Transcription factors have key role in the cytostatic effect of AICAR + MTX treatment **(A)** The genes indicated were silenced in MCF-7 cells using small interfering RNAs, targeting the indicated genes, were cloned into the pSuper vector. Control cells were transfected with the parent plasmid, pSuper. Cells were harvested 1 day post-transfection (n=4). *** indicate statistically significant difference between control and transfected samples at $p<0.001$. A typical experimental result is shown. **(B)** MCF-7 cells were seeded in 6-well plates and were transfected with the constructs indicated and were treated with AICAR and/or MTX as indicated. Treatments continued for 6 days and cells were re-transfected daily. Cellular proliferation was quantified by sulforhodamine B assay. The data is the average of 3 parallel experiments. *, ** and *** indicate statistically significant difference between control and treated cells at $p<0.05$, $p<0.01$, $p<0.001$, respectively. #, ## and ### indicate statistically significant difference between mock transfected and transfected samples (same pharmacological treatment, different construct for transfection) at $p<0.05$, $p<0.01$, $p<0.001$, respectively. All abbreviations are in the text.

6.1.6 Expression of AMPKα1 and FOXO1 positively correlate with survival in breast cancer

The previously performed experiments nominated AMPK and other mitotropic factors (PGC's, FOXO1) as possible targets in human breast cancer. To validate this possibility we screened a publicly available cancer gene expression database, (Kaplan-Meier plotter, kmplot.com). When comparing the lowest and the highest expression quartile, higher expression of AMPKα1 and FOXO1 conferred significantly longer survival to the high

expression quartile as compared to the lowest expression quartile (Figure 20). Higher expression of PGC1α did not confer longer survival (data not shown).

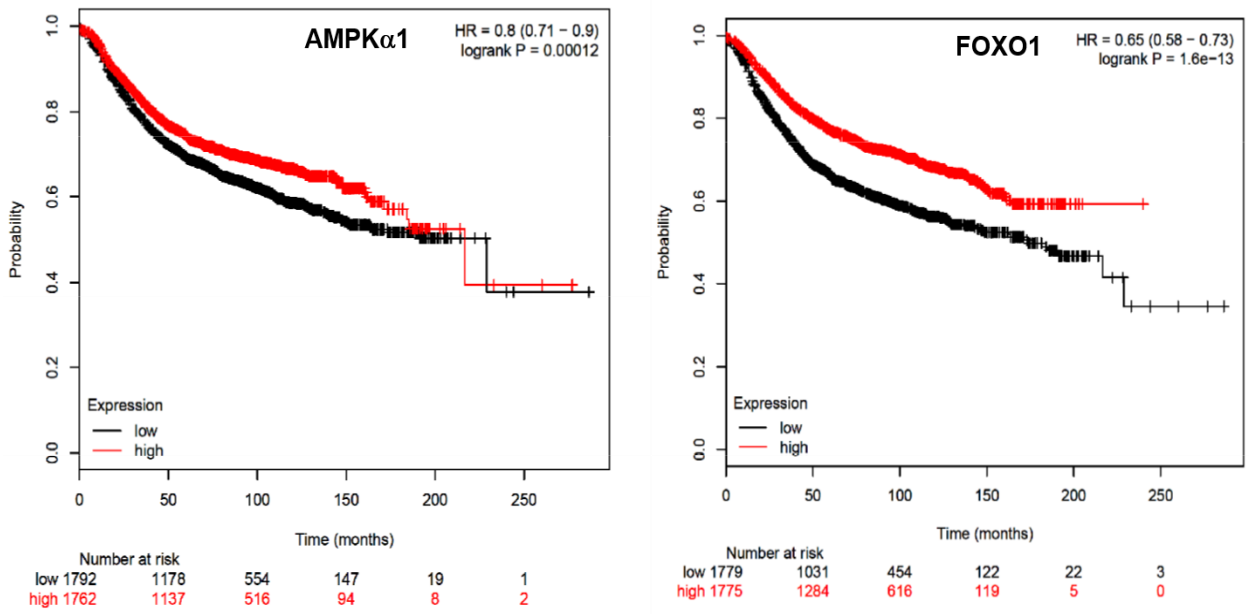

Figure 20. Mitotropic transcription factors have key role in the cytostatic effect of AICAR + MTX treatment

The kmplot.com, a freely accessible gene expression database was accessed to analyze the expression of AMPKα1 and FOXO1 on overall survival in breast cancer patients. We included all patients, also those, where ER status was derived from gene expression data. Overall survival rates were analyzed.

6.2 The role of AMPK in beige adipocyte differentiation

6.2.1 AICAR-induced AMPK activation in hADMSCs-derived white adipocytes

In our study we used hADMSC cells to model white and beige adipocytes. Each hADMSCs cell line was differentiated towards three directions: beige adipocytes, white adipocytes and AICAR-treated white adipocytes. First, we measured the AMPK activity in the three groups at the end of the differentiation. AMPK activity was higher in beige than in white adipocytes Importantly, the treatment of white adipocytes with 100 μM AICAR enhanced AMPK activity almost to the same extent as in beige adipocytes (Figure 21.) that suggested a role for AMPK in beige adipocyte differentiation and function.

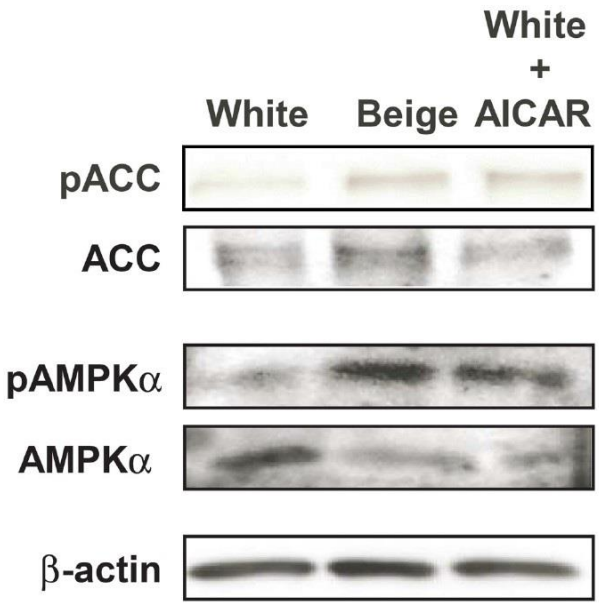

Figure 21. Measurement of AMPK activity in differentiated adipocytes.

AMPK activity measurement was performed in white, beige and white adipocytes treated with 100 µM AICAR by assessing ACC phosphorylation (pACC), total ACC, phospho-AMPKα and total AMPKα levels by Western blotting.

6.2.2 AICAR treatment of hADMSCs-derived white adipocytes does not yield functional beige adipocytes

We continued our investigation by assessing the biological functions of the beige adipocytes. Beige cells rely on the mitochondrial oxidation and mitochondrial biogenesis (Abdul-Rahman et al. 2016). As next step, we investigated the mitochondrial oxygen consumption rate. As a previous study highlighted (Kristof et al. 2015), beige adipocytes showed higher basal and cAMP-simulated oxygen consumption rate than white adipocytes. AMPK activation by AICAR did not increased the oxygen consumption rate of the white adipocytes (Figure 22).

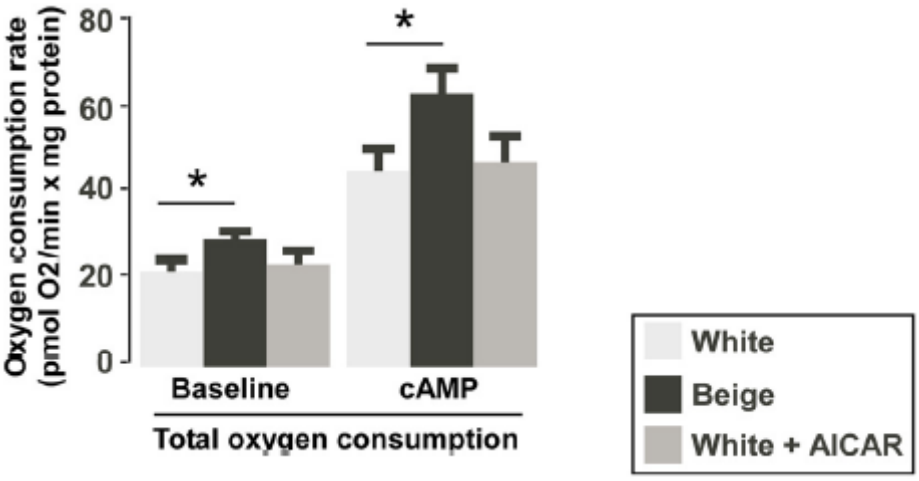

Figure 22. Determination of mitochondrial function in differentiated adipocytes

(A) Mitochondrial oxygen consumption was measured using the Seahorse XF96 oximeter (Seahorse Biosciences, North Billerica, MA, USA). One representative donor is shown (mean±SD), statistical significance was determined using the one-way ANOVA. * indicates statistically significant difference between the compared groups at $p < 0.05$

Although, the lack of the induction of OCR upon treatment with AICAR was surprising, we continued our experiments by measuring the mRNA levels some beige differentiation marker genes, Uncoupling protein-1 (UCP1), cell death-inducing DFFA-like effector A (CIDEA), PR domain containing 16 (PRDM16), transmembrane protein 26 (TMEM26) and T-box protein 1 (TBX-1). The expression levels of above-mentioned markers were higher in beige cells than in white adipose cells. We could not detect any increment upon AICAR treatment in white adipose cells (Figure 23).

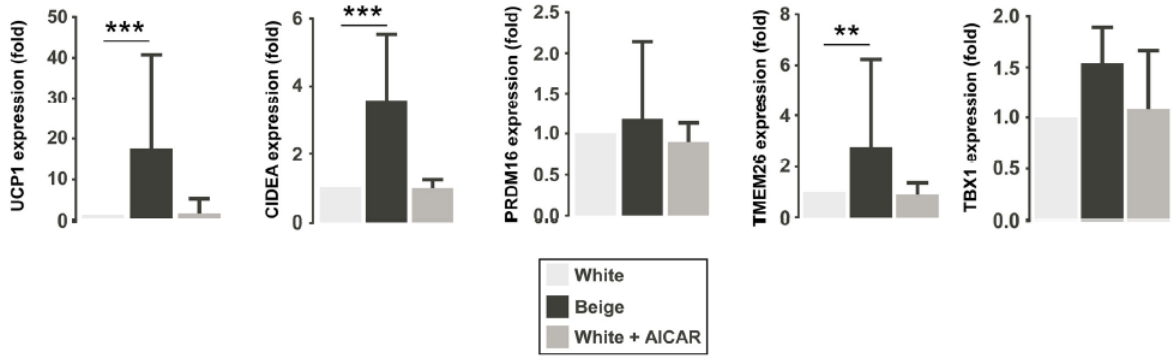

Figure 23. mRNA levels the most common beige differentiation marker genes

The expression levels of the indicated genes were determined in RT-qPCR reactions using Light-Cycler 480 system (Roche Applied Science) (n=8 except for TBX-1, where n=3, median and quartiles are plotted). Statistical significance was determined using one-way ANOVA. ** and *** indicate statistically significant difference between the indicated groups at $p<0.01$ and $p<0.001$, respectively. Abbreviations are in the text.

8. DISCUSSION

8.1 The role of AMPK in the regulation of breast cancer metabolism

In the first study we assessed whether activated AMPK is able to revert Warburg metabolism in breast cancer cells when used in combination with MTX using MCF7 invasive ductal carcinoma cell line as a model for breast cancer. We provided evidence that the AICAR+MTX combination reverted the characteristics of the Warburg phenomenon. Breast cancer is a Warburg-dependent disease, even the breast cancer initiating cells display Warburg-type metabolic alterations, namely reduced mitochondrial activity, and enhanced glycolysis and pentose phosphate shunt (Feng et al. 2014). Moreover, a recent study highlighted, that triple negative breast cancer cells also exhibit features of Warburg metabolism (Kim et al. 2013). In fact, in breast cancer, low mitochondrial activity and accelerated glycolytic flux suggest poor clinical prognosis (Isidoro et al. 2005), moreover, inducing mitochondrial activity by thyroid hormone or docosahexaenoic acid (DHA) potentiates better outcome of chemotherapy in breast cancer (Mouradian et al. 2015). A study revealed that epithelial or breast cancer cells are able to induce the aerobic glycolysis (Warburg effect) in the neighboring non–cancer stromal fibroblasts (Pavlides et al. 2009; Pavlides et al. 2012). Cancer related fibroblasts can provide energy rich metabolites for epithelial cancer cells supporting higher proliferating capacity, this process is called the reverse-Warburg effect that suggests poor outcome in patients (Pavlides et al. 2009). AMPK degradation is an initial step in Warburg metabolism (Pineda et al. 2015).

In this study we provided evidence that the combined application of the AMPK activator AICAR and antimetabolite MTX are able to potentiate each other's antiproliferative and cytostatic effects (Figure 24).

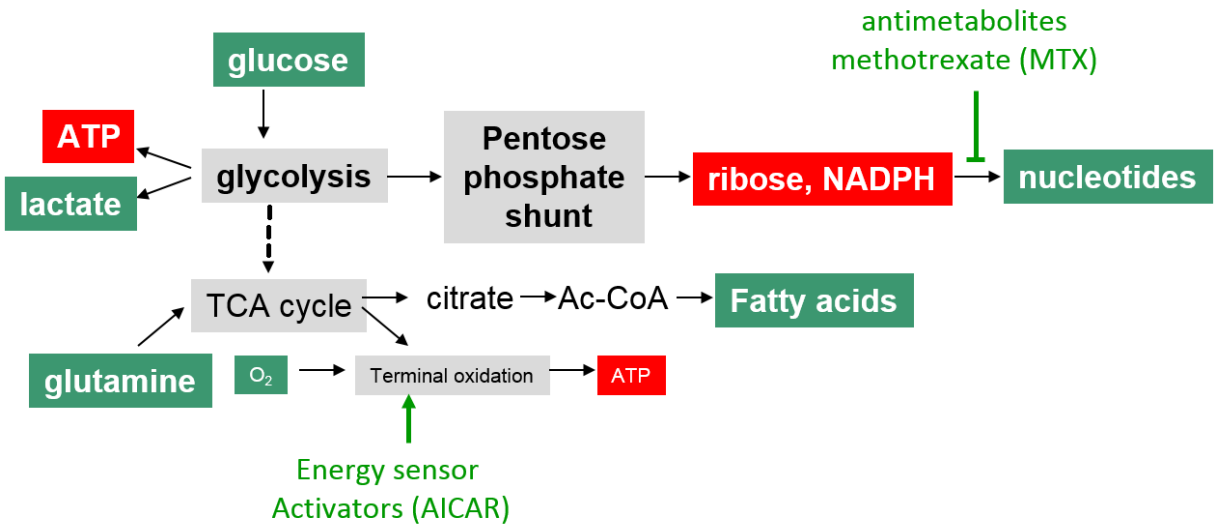

Figure 24. Energy sensor activators and antimetabolite drugs potentiate each other's effects
We inhibited nucleotide synthesis by methotrexate (MTX), a folate analog. Folate is necessary for purine base synthesis. Methotrexate acts specifically during DNA and RNA synthesis, and thus exerts cytotoxic effect in the S-phase of the cell cycle. On the other hand AICAR is capable of stimulating AMP-dependent protein kinase activity (AMPK).

We examined the consequences of short and long term AICAR+MTX treatment on MCF-7 cells. Six days long treatment of MCF-7 cells by AICAR+MTX reduced cell numbers significantly, while did not increase apoptosis or necrosis (it was not acutely toxic) suggesting that it's major mode of action was slowing down cellular proliferation. As previously highlighted, breast cancer cells rely on the Warburg metabolism (Feng et al. 2014; Ayyasamy et al. 2011; Tang et al. 2014; Suhane and Ramanujan 2011; Yadav and Chandra 2013), therefore, it is conceivable that AMPK activation stimulate mitochondrial oxidation and induces an anti-Warburg rearrangement of cellular metabolism. In line with that, prolonged AICAR+MTX treatment induced mitochondrial activity and contrary to that, decreased glycolytic rate. AMPK activation-stimulated mitochondrial biogenesis had antiproliferative effects on lymphoma *in vivo* (Faubert et al. 2013), as well as different breast cancer cells such as MCF7, SKBR-3, 4T1 (in our study) or MDA-MB-231 (Beckers et al. 2006). The models described in (Faubert et al. 2013; Beckers et al. 2006) share common features with our observations, like lower glycolytic flux and lactate production, decreased replication and proliferation rate or enhanced fatty acid oxidation and higher oxygen consumption upon AMPK activation.

We assessed how AMPK activation by AICAR+MTX can influence the cell cycle and proliferation. We observed a block at the G1 to S phase transition. There is a large set of data supporting that the G1 to S block is, at least partially, is governed by the energetic status of cells (Moncada, Higgs, and Colombo 2012). For example Colombo and colleagues

(Colombo et al. 2011) showed that Warburg metabolism supports the transition through the G1/S phase checkpoint (Colombo et al. 2011; Moncada, Higgs, and Colombo 2012).

What are the molecular pathways that regulate the events downstream of AMPK? We have observed an AICAR+MTX-dependent increase in the expression of PGC1α, PGC1β and FOXO1 that are a well characterized mitotropic transcription factors and downstream targets of AMPK (Canto et al. 2009; Lagouge et al. 2006; Rodgers et al. 2005). Importantly, the shRNA-mediated depletion of these transcription factors abolished the antiproliferative effects of AICAR+MTX treatment. The pathophysiological relevance of these findings were further strengthened by our in silico studies showing that higher expression of AMPKα1 and FOXO1 confers longer survival in breast cancer patients. A study by Faubert and colleagues (Faubert et al. 2013) suggests that AICAR treatment in lymphoma models may have other targets. Namely, AICAR suppresses HIF and mTORC1 pathways. Importantly, these pathways might be modulated in our system, too.

Our data suggest that the combined application of AICAR and MTX is an effective combination for breast cancer chemotherapy, in other words we recommend AICAR as a new synergistic agent to potentiate the MTX anti-proliferative effect. A study by Beckers and colleagues (Beckers et al. 2006) showed that AICAR+MTX combination can reduce the proliferation rate of other cancer cells like A431, a model of human squamous carcinoma (Beckers et al. 2006), suggesting that this combination may work on other cancer cells as well.

8.2 The role AMPK in the regulation of beige adipocytes differentiation

We also assessed the function of AMPK in beige cell differentiation. Beige cells morphologically phenocopy white adipocytes (monolocular fat depots), while functionally look like brown adipocytes. Beige cells reside among white adipocytes and can upregulate UCP1 expression upon adrenergic stimulation and hence generate heat. Beige adipocytes are implicated in the pathology of different metabolic diseases among others type 2 diabetes as well as heart disease, insulin resistance, hyperglycemia, dyslipidemia, hypertension and many types of cancer (Claussnitzer et al. 2015; Imran, Yoon, and Kim 2017).

Several genes are associated with the differentiation and development of beige adipocytes such as PGC1α, PRDM16, other mediator genes like BMP7, irisin and FGF21 (Harms and Seale 2013; Lo and Sun 2013; Norheim et al. 2014). Recent studies have shown that phytochemicals, like curcumin, quercetin, resveratrol and medicarpin can stimulate browning in WAT highlighted by – among others – the induction of UCP1 (Lone et al. 2016; Lee, Parks, and Kang 2017; Wang et al. 2015; Imran, Yoon, and Kim 2017). Browning induced by phytochemicals enhance the expression of transcription factors and thermogenic enzymes (Bonet, Oliver, and Palou 2013). Several investigators pointed out that β-adrenergic

activation and signal transduction can initiate the beige cells function (Seale 2015; Ye et al. 2013). In contrast to these, serotonin (5HT) was reported to decrease the thermogenic activity of BAT and beige cells in mice (Crane et al. 2015; Oh et al. 2015).

Another study pointed out that among several regulators the SIRT1-PPARγ pathway has a central role in beige adipocyte differentiation and function (Qiang et al. 2012). SIRT1 is vital for the adaptation to nutrient deprivation, fasting, or other environmental stress. SIRT1 deacetylates key transcriptional factors (PGC1α, FOXOs, p53), thereby activating them and declutching transcriptional programs that support adaptation. These transcriptional programs downregulate anabolism and activate catabolic processes and importantly upregulate mitochondrial biogenesis (Houtkooper, Pirinen, and Auwerx 2012; Imai and Guarente 2014). SIRT1 has intricate connections to other energy/metabolite sensor pathways (e.g. Akt, AMPK, HIFs, mTOR, NRFs) (Houtkooper, Pirinen, and Auwerx 2012; Imai and Guarente 2014; Bai et al. 2015; Efeyan, Comb, and Sabatini 2015; Valero 2014). SIRT1 and AMPK can regulate each other's activity (Ruderman et al. 2010) and share several common target molecules like PGC1α, FOXO1 or FOXO3. SIRT1-mediated deacetylation or AMPK-mediated phosphorylation can activate and stimulate these transcription factors. The activation of PGC1α, FOXO1 or FOXO3 culminates in mitochondrial biogenesis (Canto et al. 2009). Moreover, AMPK can regulate SIRT1 activity indirectly via the modulation of NAD^+ salvage through NAMPT (Canto et al. 2009). There are several connections between AMPK and browning or energy expenditure (Shan et al. 2013; van Dam et al. 2015; Pulinilkunnil et al. 2011; Ahmadian et al. 2011; Wang et al. 2015; Fu et al. 2014; Xin et al. 2016). For example, AMPK activation was also reported upon phytochemical-induced browning of WAT (Azhar et al. 2016). Resveratrol and curcumin activated AMPK is able to induce the browning in adipocytes characterized by elevated levels of UCP1 (Lone et al. 2016; Lee, Parks, and Kang 2017; Wang et al. 2015). Moreover, a study pointed out that overexpression of UCP-1 in skeletal muscle results in an increased AMP/ATP ratio, which consequently leads to the activation of AMPK (Neschen et al. 2008).

In our studies, the activation of AMPK by AICAR in cells differentiated to white adipocytes did induce AMPK to a comparable level as experienced in brown adipocytes, however we have not observed functional changes in the white adipocytes treated with AICAR (mitochondrial oxidation and marker gene expression). Albeit, AICAR can induce brown/beige-like changes in terms of morphology, namely, smaller lipid droplets appeared in AICAR treated WAT cells, similarly to beige cells (Figure 25).

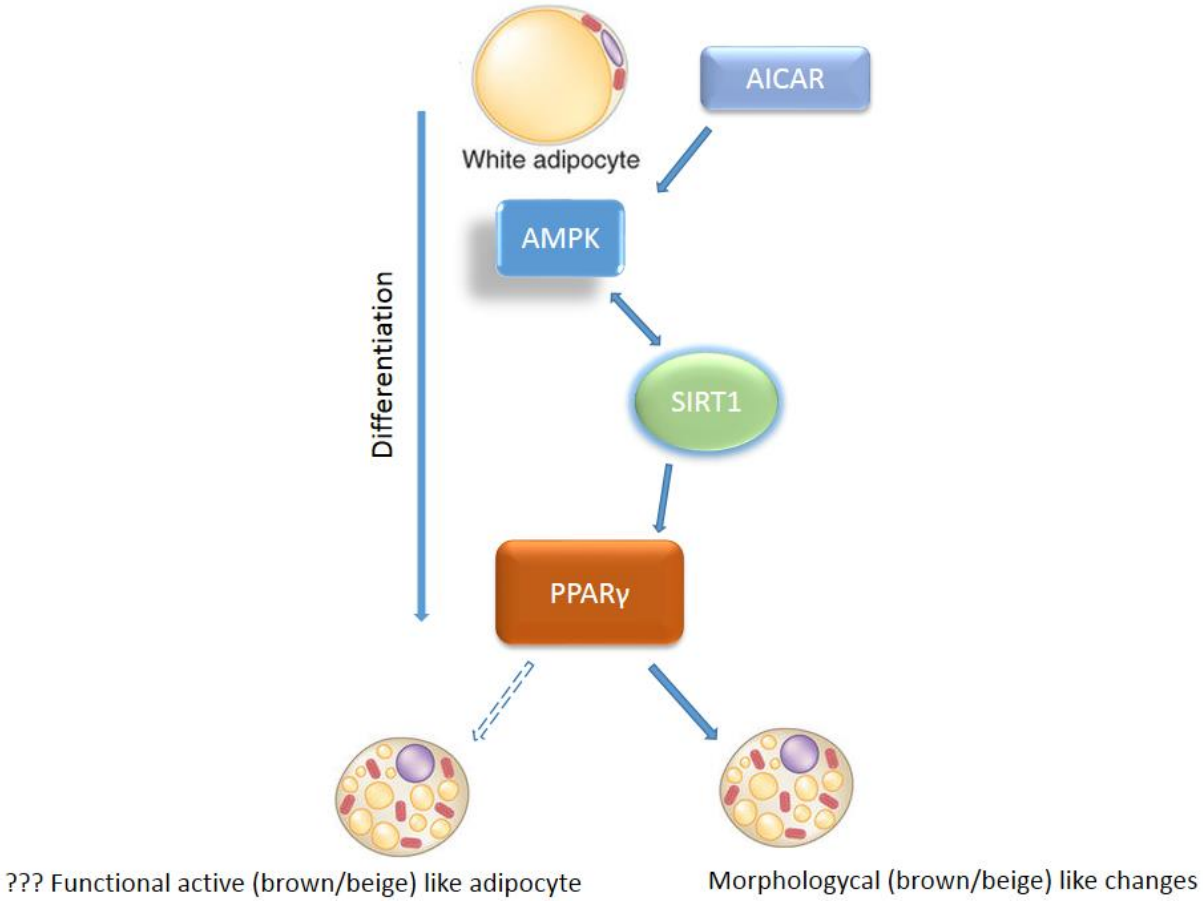

Figure 25. The role of AICAR mediated AMPK activation in adipocytes differentiation

These data suggested that AICAR induced AMPK activation in the human pericardium derived hADMSCs probably does not support the differentiation and development of functional beige cells. An alternative explanation to this observation is, that we might have used too low concentrations of AICAR and increasing AICAR concentrations could have induced more profound functional changes. Another potential explanation is that we were the first to use pericardial adipose tissue–derived stem cells that can be different than the stem cells stemming from other fat depots.

It is common in metabolic or neoplastic diseases that cells suffer from metabolic stress imitated by the altered microenvironment where AMPK activity is often down regulated. It is indispensable for cells to adapt to the changes of the microenvironment for survival. As a conclusion for both projects, we can say that AMPK activation proved to became a valuable target in the fight against metabolic and neoplastic diseases.

9. SUMMARY

The AMP-activated protein kinase (AMPK) is one of the most important energy sensor in the human body. AMPK is activated by decreases in the ATP/AMP ratio. AMPK activation has several organ or tissue specific physiological or pathological effects that all finally result in enhanced glucose and fatty acid oxidation and mitochondrial biogenesis to restore cellular ATP levels. Cancer cells often undergo metabolic alterations that can be characterized by depressed mitochondrial oxidation and enhanced glycolysis in order to support the uncontrolled and rapid cell proliferation that is called Warburg metabolism. AMPK can exert an anti-Warburg effect through enhancing of mitochondrial biogenesis. We provided evidence, that a combination of AICAR (a pharmacologic activator of AMP-activated protein kinase), together with the folate-analog methotrexate (MTX) can slow down breast cancer cell proliferation. The AICAR+MTX combination enhanced mitochondrial oxidation and reduced glycolytic rate. These metabolic alterations went together with a slowdown of the G1/S and G2/M transition that slowed down the cell cycle. The high level of expression of transcription factors, PGC1α, PGC1β, and FOXO1 were responsible for enhanced mitochondrial oxidation. The slowdown of cell proliferation was abolished when the mitochondrial transcription factors, PGC1α, PGC1β, and FOXO1 were silenced.

We also assessed the possible role of AMPK in beige cell differentiation using human adipose-derived mesenchymal stem cells (hADMSCs) originated from pericardial adipose tissue as model. In the differentiation process of hADMSCs, white adipocytes were induced by 100 μM AICAR. AICAR was able to boost AMPK activity in white adipocytes to a similar extent as in beige adipocytes. AICAR-mediated activation of AMPK did bring about morphological changes in white adipocytes similar to the one in beige adipocytes. However, we were unable to detect functional changes in the AICAR-treated white adipocytes. Neither mitochondrial oxidation, nor the expression of marker genes (TBX1, UCP1, CIDEA, PRDM16 and TMEM26) was comparable to that in brown adipocytes.

Our experiments provided evidence that AICAR-induced AMPK activation has an exploitable potential in treating metabolic and neoplastic diseases.

10. ÖSZEFOGLALÁS

Az AMP-aktivált protein kináz egyike az emberi szervezet legfontosabb energiaszenzorainak. Működését az ATP/AMP arány szabályozza. Az enzim egy heterotrimer, amelynek gamma alegysége AMP-t köt, amely az enzim aktivációjához vezet. Tulajdonképpen az AMPK aktiváció a magas AMP szinthez kötött, azaz a sejtek energetikai stresszének a következménye. Az AMPK akkor aktiválódik, ha valamilyen eltérés áll be a sejt tápláltsági alapállapotban. Az AMPK aktivációja több szerv és szövetfüggő hatást vált ki. E hatásokban közös, hogy beindítják a cukor és a zsírsav oxidációt, hogy helyreállítsák a sejtek, szövetek ATP szintjét. A rákos sejtek olyan metabolikus változásokon mennek keresztül, ami csökkent mitokondriális oxidációval és emelkedett glikolitikus rátával jellemezhető. Ez a Warburg metabolizmusnak nevezett állapot a gyors és kontrollálatlan sejtproliferáció szolgálatában áll. Az AMPK a mitokondriális biogenezis fokozásán keresztül anti-Warburg szerként képes viselkedni. Bizonyítottuk, hogy az AMP aktivált protein kináz farmakológiai aktivátora (AICAR) és a folát analóg metotrexát (MTX) együttes alkalmazása lelassíthatja az emlő tumor sejtek proliferációját. Az AICAR+MTX kombináció fokozott mitokondriális oxidációt és csökkent glikolítikus rátát eredményezett. Ezek a metabolikus változások együtt jártak a G1/S és a G2/M fázisok közötti átmenet blokkolásával, amely lelassította a sejtciklust.

A PGC1α, PGC1β, és FOXO1 transzkripciós faktorok expressziójának magas szintje felelős a fokozott mitokondriális oxidációért. A sejtproliferáció lassulása megszűnt, amikor a mitokondriális transzkripciós faktorokat csendesítettük.

További kísérleteinkben meghatároztuk az AMPK lehetséges szerepét a bézs sejtek differenciációjában, amelyhez humán perikardiális zsírszövetből származó mesenchymalis őssejteket (hADMSC) használtunk modellként. A hADMSC-k differenciálódási folyamatában a fehér zsírsejteket 100 μM AICAR-val indukáltuk. Azt tapasztaltuk, hogy az AICAR képes volt növelni az AMPK aktivitást a fehér zsírszövetben hasonló mértékben, mint a bézs adipocitákban. Az AICAR által indukált AMPK aktivitás morfológiai változásokat eredményezett a fehér zsírsejtekben, hasonlóan a barna adipocitákhoz. Viszont az AICAR kezelt fehér adipocitákban nem tudtunk funkcionális változásokat kimutatni, sem a mitokondriális oxidáció, sem a bézs zsírsejtekre jellemző marker gének (TBX1, UCP1, CIDEA, PRDM16 és TMEM26) expressziójának vizsgálatakor, összehasonlítva a bézs adipocitákkal.

Kísérleteink azt bizonyítják, hogy az AICAR által indukált AMPK aktiváció kiemelkedő potenciállal rendelkezik az anyagcsere és a daganatos megbetegedések kezelésében.

11. REFERENCES

Abdul-Rahman, O., E. Kristof, Q. M. Doan-Xuan, A. Vida, L. Nagy, A. Horvath, J. Simon, T. Maros, I. Szentkiralyi, L. Palotas, T. Debreceni, P. Csizmadia, T. Szerafin, T. Fodor, M. Szanto, A. Toth, B. Kiss, Z. Bacso, and P. Bai. 2016. 'AMP-Activated Kinase (AMPK) Activation by AICAR in Human White Adipocytes Derived from Pericardial White Adipose Tissue Stem Cells Induces a Partial Beige-Like Phenotype', *PLoS One*, 11: e0157644.

Adams, J., Z. P. Chen, B. J. Van Denderen, C. J. Morton, M. W. Parker, L. A. Witters, D. Stapleton, and B. E. Kemp. 2004. 'Intrasteric control of AMPK via the gamma1 subunit AMP allosteric regulatory site', *Protein Sci*, 13: 155-65.

Ahmadian, M., M. J. Abbott, T. Tang, C. S. Hudak, Y. Kim, M. Bruss, M. K. Hellerstein, H. Y. Lee, V. T. Samuel, G. I. Shulman, Y. Wang, R. E. Duncan, C. Kang, and H. S. Sul. 2011. 'Desnutrin/ATGL is regulated by AMPK and is required for a brown adipose phenotype', *Cell Metab*, 13: 739-48.

Amann, R., and B. A. Peskar. 2002. 'Anti-inflammatory effects of aspirin and sodium salicylate', *Eur J Pharmacol*, 447: 1-9.

Andrade-Vieira, R., D. Goguen, H. A. Bentley, C. V. Bowen, and P. A. Marignani. 2014. 'Pre-clinical study of drug combinations that reduce breast cancer burden due to aberrant mTOR and metabolism promoted by LKB1 loss', *Oncotarget*, 5: 12738-52.

Auwerx, J. 2006. 'Improving metabolism by increasing energy expenditure', *Nat Med*, 12: 44-5; discussion 45.

Ayyasamy, V., K. M. Owens, M. M. Desouki, P. Liang, A. Bakin, K. Thangaraj, D. J. Buchsbaum, A. F. LoBuglio, and K. K. Singh. 2011. 'Cellular model of Warburg effect identifies tumor promoting function of UCP2 in breast cancer and its suppression by genipin', *PLoS One*, 6: e24792.

Azhar, Y., A. Parmar, C. N. Miller, J. S. Samuels, and S. Rayalam. 2016. 'Phytochemicals as novel agents for the induction of browning in white adipose tissue', *Nutr Metab (Lond)*, 13: 89.

Bai, P., E. Bakondi, E. Szabo, P. Gergely, C. Szabo, and L. Virag. 2001. 'Partial protection by poly(ADP-ribose) polymerase inhibitors from nitroxyl-induced cytotoxity in thymocytes', *Free Radic Biol Med*, 31: 1616-23.

Bai, P., S. M. Houten, A. Huber, V. Schreiber, M. Watanabe, B. Kiss, G. de Murcia, J. Auwerx, and J. Menissier-de Murcia. 2007. 'Poly(ADP-ribose) polymerase-2 [corrected] controls adipocyte differentiation and adipose tissue function through the regulation of the activity of the retinoid X receptor/peroxisome proliferator-activated receptor-gamma [corrected] heterodimer', *J Biol Chem*, 282: 37738-46.

Bai, P., L. Nagy, T. Fodor, L. Liaudet, and P. Pacher. 2015. 'Poly(ADP-ribose) polymerases as modulators of mitochondrial activity', *Trends Endocrinol Metab*, 26: 75-83.

Bartelt, A., and J. Heeren. 2014. 'Adipose tissue browning and metabolic health', *Nat Rev Endocrinol*, 10: 24-36.

Baur, J. A., D. Chen, E. N. Chini, K. Chua, H. Y. Cohen, R. de Cabo, C. Deng, S. Dimmeler, D. Gius, L. P. Guarente, S. L. Helfand, S. Imai, H. Itoh, T. Kadowaki, D. Koya, C. Leeuwenburgh, M. McBurney, Y. Nabeshima, C. Neri, P. Oberdoerffer, R. G. Pestell, B. Rogina, J. Sadoshima, V. Sartorelli, M. Serrano, D. A. Sinclair, C. Steegborn, M. Tatar, H. A. Tissenbaum, Q. Tong, K. Tsubota, A. Vaquero, and E. Verdin. 2010. 'Dietary restriction: standing up for sirtuins', *Science*, 329: 1012-3; author reply 13-4.

Beckers, A., S. Organe, L. Timmermans, F. Vanderhoydonc, L. Deboel, R. Derua, E. Waelkens, K. Brusselmans, G. Verhoeven, and J. V. Swinnen. 2006. 'Methotrexate enhances the antianabolic and antiproliferative effects of 5-aminoimidazole-4-carboxamide riboside', *Mol Cancer Ther*, 5: 2211-7.

Bevers, T. B., B. O. Anderson, E. Bonaccio, S. Buys, M. B. Daly, P. J. Dempsey, W. B. Farrar, I. Fleming, J. E. Garber, R. E. Harris, A. S. Heerdt, M. Helvie, J. G. Huff, N. Khakpour, S. A. Khan, H. Krontiras, G. Lyman, E. Rafferty, S. Shaw, M. L. Smith, T. N. Tsangaris, C. Williams, and T. Yankeelov. 2009. 'NCCN clinical practice guidelines in oncology: breast cancer screening and diagnosis', *J Natl Compr Canc Netw*, 7: 1060-96.

Birnbaum, M. J. 2005. 'Activating AMP-activated protein kinase without AMP', *Mol Cell*, 19: 289-90.

Bitterman, K. J., R. M. Anderson, H. Y. Cohen, M. Latorre-Esteves, and D. A. Sinclair. 2002. 'Inhibition of silencing and accelerated aging by nicotinamide, a putative negative regulator of yeast sir2 and human SIRT1', *J Biol Chem*, 277: 45099-107.

Bonet, M. L., P. Oliver, and A. Palou. 2013. 'Pharmacological and nutritional agents promoting browning of white adipose tissue', *Biochim Biophys Acta*, 1831: 969-85.

Brunet, A., L. B. Sweeney, J. F. Sturgill, K. F. Chua, P. L. Greer, Y. Lin, H. Tran, S. E. Ross, R. Mostoslavsky, H. Y. Cohen, L. S. Hu, H. L. Cheng, M. P. Jedrychowski, S. P. Gygi, D. A. Sinclair, F. W. Alt, and M. E. Greenberg. 2004. 'Stress-dependent regulation of FOXO transcription factors by the SIRT1 deacetylase', *Science*, 303: 2011-5.

Cannon, B., and J. Nedergaard. 2004. 'Brown adipose tissue: function and physiological significance', *Physiol Rev*, 84: 277-359.

Canto, C., and J. Auwerx. 2010. 'AMP-activated protein kinase and its downstream transcriptional pathways', *Cell Mol Life Sci*, 67: 3407-23.

Canto, C., Z. Gerhart-Hines, J. N. Feige, M. Lagouge, L. Noriega, J. C. Milne, P. J. Elliott, P. Puigserver, and J. Auwerx. 2009. 'AMPK regulates energy expenditure by modulating NAD+ metabolism and SIRT1 activity', *Nature*, 458: 1056-60.

Carling, D., and D. G. Hardie. 1989. 'The substrate and sequence specificity of the AMP-activated protein kinase. Phosphorylation of glycogen synthase and phosphorylase kinase', *Biochim Biophys Acta*, 1012: 81-6.

Carling, D., M. J. Sanders, and A. Woods. 2008. 'The regulation of AMP-activated protein kinase by upstream kinases', *Int J Obes (Lond)*, 32 Suppl 4: S55-9.

Christian, M. 2015. 'Transcriptional fingerprinting of "browning" white fat identifies NRG4 as a novel adipokine', *Adipocyte*, 4: 50-4.

Claussnitzer, M., S. N. Dankel, K. H. Kim, G. Quon, W. Meuleman, C. Haugen, V. Glunk, I. S. Sousa, J. L. Beaudry, V. Puviindran, N. A. Abdennur, J. Liu, P. A. Svensson, Y. H. Hsu, D. J. Drucker, G. Mellgren, C. C. Hui, H. Hauner, and M. Kellis. 2015. 'FTO Obesity Variant Circuitry and Adipocyte Browning in Humans', *N Engl J Med*, 373: 895-907.

Colman, R. J., R. M. Anderson, S. C. Johnson, E. K. Kastman, K. J. Kosmatka, T. M. Beasley, D. B. Allison, C. Cruzen, H. A. Simmons, J. W. Kemnitz, and R. Weindruch. 2009. 'Caloric restriction delays disease onset and mortality in rhesus monkeys', *Science*, 325: 201-4.

Colombo, S. L., M. Palacios-Callender, N. Frakich, S. Carcamo, I. Kovacs, S. Tudzarova, and S. Moncada. 2011. 'Molecular basis for the differential use of glucose and glutamine in cell proliferation as revealed by synchronized HeLa cells', *Proc Natl Acad Sci U S A*, 108: 21069-74.

Corton, J. M., J. G. Gillespie, S. A. Hawley, and D. G. Hardie. 1995. '5-aminoimidazole-4-carboxamide ribonucleoside. A specific method for activating AMP-activated protein kinase in intact cells?', *Eur J Biochem*, 229: 558-65.

Coughlan, K. A., R. J. Valentine, N. B. Ruderman, and A. K. Saha. 2013. 'Nutrient Excess in AMPK Downregulation and Insulin Resistance', *J Endocrinol Diabetes Obes*, 1: 1008.

Crane, J. D., R. Palanivel, E. P. Mottillo, A. L. Bujak, H. Wang, R. J. Ford, A. Collins, R. M. Blumer, M. D. Fullerton, J. M. Yabut, J. J. Kim, J. E. Ghia, S. M. Hamza, K. M. Morrison, J. D. Schertzer, J. R. Dyck, W. I. Khan, and G. R. Steinberg. 2015. 'Inhibiting peripheral serotonin synthesis reduces obesity and metabolic dysfunction by promoting brown adipose tissue thermogenesis', *Nat Med*, 21: 166-72.

Dakubo, Gabriel D. 2010. 'The Warburg Phenomenon and Other Metabolic Alterations of Cancer Cells.' in, *Mitochondrial Genetics and Cancer* (Springer Berlin Heidelberg: Berlin, Heidelberg).

Davies, S. P., N. R. Helps, P. T. Cohen, and D. G. Hardie. 1995. '5'-AMP inhibits dephosphorylation, as well as promoting phosphorylation, of the AMP-activated protein kinase. Studies using bacterially expressed human protein phosphatase-2C alpha and native bovine protein phosphatase-2AC', *FEBS Lett*, 377: 421-5.

DeBerardinis, R. J., J. J. Lum, G. Hatzivassiliou, and C. B. Thompson. 2008. 'The biology of cancer: metabolic reprogramming fuels cell growth and proliferation', *Cell Metab*, 7: 11-20.

Efeyan, A., W. C. Comb, and D. M. Sabatini. 2015. 'Nutrient-sensing mechanisms and pathways', *Nature*, 517: 302-10.

Elabd, C., C. Chiellini, M. Carmona, J. Galitzky, O. Cochet, R. Petersen, L. Penicaud, K. Kristiansen, A. Bouloumie, L. Casteilla, C. Dani, G. Ailhaud, and E. Z. Amri. 2009. 'Human multipotent adipose-derived stem cells differentiate into functional brown adipocytes', *Stem Cells*, 27: 2753-60.

Faubert, B., G. Boily, S. Izreig, T. Griss, B. Samborska, Z. Dong, F. Dupuy, C. Chambers, B. J. Fuerth, B. Viollet, O. A. Mamer, D. Avizonis, R. J. DeBerardinis, P. M. Siegel, and R. G. Jones. 2013. 'AMPK is a negative regulator of the Warburg effect and suppresses tumor growth in vivo', *Cell Metab*, 17: 113-24.

Favaro, E., K. Bensaad, M. G. Chong, D. A. Tennant, D. J. Ferguson, C. Snell, G. Steers, H. Turley, J. L. Li, U. L. Gunther, F. M. Buffa, A. McIntyre, and A. L. Harris. 2012. 'Glucose Utilization via Glycogen Phosphorylase Sustains Proliferation and Prevents Premature Senescence in Cancer Cells', *Cell Metab*, 16: 751-64.

Feng, W., A. Gentles, R. V. Nair, M. Huang, Y. Lin, C. Y. Lee, S. Cai, F. A. Scheeren, A. H. Kuo, and M. Diehn. 2014. 'Targeting unique metabolic properties of breast tumor initiating cells', *Stem Cells*, 32: 1734-45.

Ferlay, J., I. Soerjomataram, R. Dikshit, S. Eser, C. Mathers, M. Rebelo, D. M. Parkin, D. Forman, and F. Bray. 2015. 'Cancer incidence and mortality worldwide: sources, methods and major patterns in GLOBOCAN 2012', *Int J Cancer*, 136: E359-86.

Fernandez-Marcos, P. J., and J. Auwerx. 2011. 'Regulation of PGC1alpha, a nodal regulator of mitochondrial biogenesis', *Am J Clin Nutr*, 93: 884s-90.

Fischer-Posovszky, P., F. S. Newell, M. Wabitsch, and H. E. Tornqvist. 2008. 'Human SGBS cells - a unique tool for studies of human fat cell biology', *Obes Facts*, 1: 184-9.

Fontana, L., L. Partridge, and V. D. Longo. 2010. 'Extending healthy life span--from yeast to humans', *Science*, 328: 321-6.

Fu, T., S. Seok, S. Choi, Z. Huang, K. Suino-Powell, H. E. Xu, B. Kemper, and J. K. Kemper. 2014. 'MicroRNA 34a inhibits beige and brown fat formation in obesity in part by suppressing adipocyte fibroblast growth factor 21 signaling and SIRT1 function', *Mol Cell Biol*, 34: 4130-42.

Fulco, M., Y. Cen, P. Zhao, E. P. Hoffman, M. W. McBurney, A. A. Sauve, and V. Sartorelli. 2008. 'Glucose restriction inhibits skeletal myoblast differentiation by activating SIRT1 through AMPK-mediated regulation of Nampt', *Dev Cell*, 14: 661-73.

Gan, R. Y., and H. B. Li. 2014. 'Recent progress on liver kinase B1 (LKB1): expression, regulation, downstream signaling and cancer suppressive function', *Int J Mol Sci*, 15: 16698-718.

Garruti, G., and D. Ricquier. 1992. 'Analysis of uncoupling protein and its mRNA in adipose tissue deposits of adult humans', *Int J Obes Relat Metab Disord*, 16: 383-90.

Gerhart-Hines, Z., J. T. Rodgers, O. Bare, C. Lerin, S. H. Kim, R. Mostoslavsky, F. W. Alt, Z. Wu, and P. Puigserver. 2007. 'Metabolic control of muscle mitochondrial function and fatty acid oxidation through SIRT1/PGC1alpha', *Embo j*, 26: 1913-23.

Grahame Hardie, D. 2016. 'Regulation of AMP-activated protein kinase by natural and synthetic activators', *Acta Pharm Sin B*, 6: 1-19.

Green, D. R., L. Galluzzi, and G. Kroemer. 2014. 'Cell biology. Metabolic control of cell death', *Science*, 345: 1250256.

Greer, E. L., M. R. Banko, and A. Brunet. 2009. 'AMP-activated protein kinase and FoxO transcription factors in dietary restriction-induced longevity', *Ann N Y Acad Sci*, 1170: 688-92.

Gustafson, B., A. Hammarstedt, S. Hedjazifar, J. M. Hoffmann, P. A. Svensson, J. Grimsby, C. Rondinone, and U. Smith. 2015. 'BMP4 and BMP Antagonists Regulate Human White and Beige Adipogenesis', *Diabetes*, 64: 1670-81.

Halse, R., L. G. Fryer, J. G. McCormack, D. Carling, and S. J. Yeaman. 2003. 'Regulation of glycogen synthase by glucose and glycogen: a possible role for AMP-activated protein kinase', *Diabetes*, 52: 9-15.

Hardie, D. G. 2007. 'AMP-activated/SNF1 protein kinases: conserved guardians of cellular energy', *Nat Rev Mol Cell Biol*, 8: 774-85.

Hardie, D. G., and D. R. Alessi. 2013. 'LKB1 and AMPK and the cancer-metabolism link - ten years after', *BMC Biol*, 11: 36.

Hardie, D. G., and D. A. Pan. 2002. 'Regulation of fatty acid synthesis and oxidation by the AMP-activated protein kinase', *Biochem Soc Trans*, 30: 1064-70.

Harms, M., and P. Seale. 2013. 'Brown and beige fat: development, function and therapeutic potential', *Nat Med*, 19: 1252-63.

Hawley, S. A., M. D. Fullerton, F. A. Ross, J. D. Schertzer, C. Chevtzoff, K. J. Walker, M. W. Peggie, D. Zibrova, K. A. Green, K. J. Mustard, B. E. Kemp, K. Sakamoto, G. R. Steinberg, and D. G. Hardie. 2012. 'The ancient drug salicylate directly activates AMP-activated protein kinase', *Science*, 336: 918-22.

Houtkooper, R. H., E. Pirinen, and J. Auwerx. 2012. 'Sirtuins as regulators of metabolism and healthspan', *Nat Rev Mol Cell Biol*, 13: 225-38.

Hsu, P. P., and D. M. Sabatini. 2008. 'Cancer cell metabolism: Warburg and beyond', *Cell*, 134: 703-7.

Huss, J. M., R. P. Kopp, and D. P. Kelly. 2002. 'Peroxisome proliferator-activated receptor coactivator-1alpha (PGC1alpha) coactivates the cardiac-enriched nuclear receptors estrogen-related receptor-alpha and -gamma. Identification of novel leucine-rich interaction motif within PGC1alpha', *J Biol Chem*, 277: 40265-74.

Icard, P., and H. Lincet. 2012. 'A global view of the biochemical pathways involved in the regulation of the metabolism of cancer cells', *Biochim Biophys Acta*, 1826: 423-33.

Imai, S., and L. Guarente. 2014. 'NAD+ and sirtuins in aging and disease', *Trends Cell Biol*, 24: 464-71.

Imran, K. M., D. Yoon, and Y. S. Kim. 2017. 'A pivotal role of AMPK signaling in medicarpin-mediated formation of brown and beige adipocytes from C3H10T1/2 mesenchymal stem cells', *Biofactors*.

Inagaki, T., J. Sakai, and S. Kajimura. 2017. 'Transcriptional and epigenetic control of brown and beige adipose cell fate and function', *Nat Rev Mol Cell Biol*, 18: 527.

Inokuchi-Shimizu, S., E. J. Park, Y. S. Roh, L. Yang, B. Zhang, J. Song, S. Liang, M. Pimienta, K. Taniguchi, X. Wu, K. Asahina, W. Lagakos, M. R. Mackey, S. Akira, M. H. Ellisman, D. D. Sears, J. M. Olefsky, M. Karin, D. A. Brenner, and E. Seki. 2014. 'TAK1-mediated autophagy and fatty acid oxidation prevent hepatosteatosis and tumorigenesis', *J Clin Invest*, 124: 3566-78.

Isidoro, A., E. Casado, A. Redondo, P. Acebo, E. Espinosa, A. M. Alonso, P. Cejas, D. Hardisson, J. A. Fresno Vara, C. Belda-Iniesta, M. Gonzalez-Baron, and J. M. Cuezva. 2005. 'Breast carcinomas fulfill the Warburg hypothesis and provide metabolic markers of cancer prognosis', *Carcinogenesis*, 26: 2095-104.

Jager, S., C. Handschin, J. St-Pierre, and B. M. Spiegelman. 2007. 'AMP-activated protein kinase (AMPK) action in skeletal muscle via direct phosphorylation of PGC1alpha', *Proc Natl Acad Sci U S A*, 104: 12017-22.

Jeon, S. M. 2016. 'Regulation and function of AMPK in physiology and diseases', *Exp Mol Med*, 48: e245.

Kahn, B. B., T. Alquier, D. Carling, and D. G. Hardie. 2005. 'AMP-activated protein kinase: ancient energy gauge provides clues to modern understanding of metabolism', *Cell Metab*, 1: 15-25.

Kazak, L., E. T. Chouchani, M. P. Jedrychowski, B. K. Erickson, K. Shinoda, P. Cohen, R. Vetrivelan, G. Z. Lu, D. Laznik-Bogoslavski, S. C. Hasenfuss, S. Kajimura, S. P. Gygi, and B. M. Spiegelman. 2015. 'A creatine-driven substrate cycle enhances energy expenditure and thermogenesis in beige fat', *Cell*, 163: 643-55.

Kim, S., D. H. Kim, W. H. Jung, and J. S. Koo. 2013. 'Metabolic phenotypes in triple-negative breast cancer', *Tumour Biol*, 34: 1699-712.

Kim, S. Y., S. Jeong, E. Jung, K. H. Baik, M. H. Chang, S. A. Kim, J. H. Shim, E. Chun, and K. Y. Lee. 2012. 'AMP-activated protein kinase-alpha1 as an activating kinase of TGF-beta-activated kinase 1 has a key role in inflammatory signals', *Cell Death Dis*, 3: e357.

Kola, B., E. Hubina, S. A. Tucci, T. C. Kirkham, E. A. Garcia, S. E. Mitchell, L. M. Williams, S. A. Hawley, D. G. Hardie, A. B. Grossman, and M. Korbonits. 2005. 'Cannabinoids and ghrelin have both central and peripheral metabolic and cardiac effects via AMP-activated protein kinase', *J Biol Chem*, 280: 25196-201.

Korsse, S. E., M. P. Peppelenbosch, and W. van Veelen. 2013. 'Targeting LKB1 signaling in cancer', *Biochim Biophys Acta*, 1835: 194-210.

Kristof, E., Q. M. Doan-Xuan, P. Bai, Z. Bacso, and L. Fesus. 2015. 'Laser-scanning cytometry can quantify human adipocyte browning and proves effectiveness of irisin', *Sci Rep*, 5: 12540.

Kurth-Kraczek, E. J., M. F. Hirshman, L. J. Goodyear, and W. W. Winder. 1999. '5' AMP-activated protein kinase activation causes GLUT4 translocation in skeletal muscle', *Diabetes*, 48: 1667-71.

Laderoute, K. R., K. Amin, J. M. Calaoagan, M. Knapp, T. Le, J. Orduna, M. Foretz, and B. Viollet. 2006. '5'-AMP-activated protein kinase (AMPK) is induced by low-oxygen and glucose deprivation conditions found in solid-tumor microenvironments', *Mol Cell Biol*, 26: 5336-47.

Lagouge, M., C. Argmann, Z. Gerhart-Hines, H. Meziane, C. Lerin, F. Daussin, N. Messadeq, J. Milne, P. Lambert, P. Elliott, B. Geny, M. Laakso, P. Puigserver, and J. Auwerx. 2006. 'Resveratrol improves mitochondrial function and protects against metabolic disease by activating SIRT1 and PGC1alpha', *Cell*, 127: 1109-22.

Lai, L., T. C. Leone, C. Zechner, P. J. Schaeffer, S. M. Kelly, D. P. Flanagan, D. M. Medeiros, A. Kovacs, and D. P. Kelly. 2008. 'Transcriptional coactivators PGC1alpha and PGC-lbeta control overlapping programs required for perinatal maturation of the heart', *Genes Dev*, 22: 1948-61.

Lan, F., J. M. Cacicedo, N. Ruderman, and Y. Ido. 2008. 'SIRT1 modulation of the acetylation status, cytosolic localization, and activity of LKB1. Possible role in AMP-activated protein kinase activation', *J Biol Chem*, 283: 27628-35.

Lee, S. G., J. S. Parks, and H. W. Kang. 2017. 'Quercetin, a functional compound of onion peel, remodels white adipocytes to brown-like adipocytes', *J Nutr Biochem*, 42: 62-71.

Lipovka, Y., and J. P. Konhilas. 2015. 'AMP-Activated Protein Kinase Signalling in Cancer and Cardiac Hypertrophy', *Cardiovasc Pharm Open Access*, 4.

Lo, K. A., and L. Sun. 2013. 'Turning WAT into BAT: a review on regulators controlling the browning of white adipocytes', *Biosci Rep*, 33.

Lone, J., J. H. Choi, S. W. Kim, and J. W. Yun. 2016. 'Curcumin induces brown fat-like phenotype in 3T3-L1 and primary white adipocytes', *J Nutr Biochem*, 27: 193-202.

Long, Y. C., and J. R. Zierath. 2006. 'AMP-activated protein kinase signaling in metabolic regulation', *J Clin Invest*, 116: 1776-83.

Lopez, M., C. Dieguez, and R. Nogueiras. 2015. 'Hypothalamic GLP-1: the control of BAT thermogenesis and browning of white fat', *Adipocyte*, 4: 141-5.

Marsin, A. S., L. Bertrand, M. H. Rider, J. Deprez, C. Beauloye, M. F. Vincent, G. Van den Berghe, D. Carling, and L. Hue. 2000. 'Phosphorylation and activation of heart PFK-2 by AMPK has a role in the stimulation of glycolysis during ischaemia', *Curr Biol*, 10: 1247-55.

McGlashon, J. M., M. C. Gorecki, A. E. Kozlowski, C. K. Thirnbeck, K. R. Markan, K. L. Leslie, M. E. Kotas, M. J. Potthoff, G. B. Richerson, and M. P. Gillum. 2015. 'Central

serotonergic neurons activate and recruit thermogenic brown and beige fat and regulate glucose and lipid homeostasis', *Cell Metab*, 21: 692-705.
Merrill, G. F., E. J. Kurth, D. G. Hardie, and W. W. Winder. 1997. 'AICA riboside increases AMP-activated protein kinase, fatty acid oxidation, and glucose uptake in rat muscle', *Am J Physiol*, 273: E1107-12.
Michan, S., and D. Sinclair. 2007. 'Sirtuins in mammals: insights into their biological function', *Biochem J*, 404: 1-13.
Mills, S. E., D. W. Foster, and J. D. McGarry. 1983. 'Interaction of malonyl-CoA and related compounds with mitochondria from different rat tissues. Relationship between ligand binding and inhibition of carnitine palmitoyltransferase I', *Biochem J*, 214: 83-91.
Minokoshi, Y., T. Alquier, N. Furukawa, Y. B. Kim, A. Lee, B. Xue, J. Mu, F. Foufelle, P. Ferre, M. J. Birnbaum, B. J. Stuck, and B. B. Kahn. 2004. 'AMP-kinase regulates food intake by responding to hormonal and nutrient signals in the hypothalamus', *Nature*, 428: 569-74.
Minokoshi, Y., Y. B. Kim, O. D. Peroni, L. G. Fryer, C. Muller, D. Carling, and B. B. Kahn. 2002. 'Leptin stimulates fatty-acid oxidation by activating AMP-activated protein kinase', *Nature*, 415: 339-43.
Moffat, C., and M. E. Harper. 2010. 'Metabolic functions of AMPK: aspects of structure and of natural mutations in the regulatory gamma subunits', *IUBMB Life*, 62: 739-45.
Momcilovic, M., S. P. Hong, and M. Carlson. 2006. 'Mammalian TAK1 activates Snf1 protein kinase in yeast and phosphorylates AMP-activated protein kinase in vitro', *J Biol Chem*, 281: 25336-43.
Moncada, S., E. A. Higgs, and S. L. Colombo. 2012. 'Fulfilling the metabolic requirements for cell proliferation', *Biochem J*, 446: 1-7.
Mouradian, M., K. D. Kikawa, B. P. Dranka, S. M. Komas, B. Kalyanaraman, and R. S. Pardini. 2015. 'Docosahexaenoic acid attenuates breast cancer cell metabolism and the Warburg phenotype by targeting bioenergetic function', *Mol Carcinog*, 54: 810-20.
Mungai, P. T., G. B. Waypa, A. Jairaman, M. Prakriya, D. Dokic, M. K. Ball, and P. T. Schumacker. 2011. 'Hypoxia triggers AMPK activation through reactive oxygen species-mediated activation of calcium release-activated calcium channels', *Mol Cell Biol*, 31: 3531-45.
Nakashima, K., and Y. Yakabe. 2007. 'AMPK activation stimulates myofibrillar protein degradation and expression of atrophy-related ubiquitin ligases by increasing FOXO transcription factors in C2C12 myotubes', *Biosci Biotechnol Biochem*, 71: 1650-6.
Narkar, V. A., M. Downes, R. T. Yu, E. Embler, Y. X. Wang, E. Banayo, M. M. Mihaylova, M. C. Nelson, Y. Zou, H. Juguilon, H. Kang, R. J. Shaw, and R. M. Evans. 2008. 'AMPK and PPARdelta agonists are exercise mimetics', *Cell*, 134: 405-15.
Neschen, S., Y. Katterle, J. Richter, R. Augustin, S. Scherneck, F. Mirhashemi, A. Schurmann, H. G. Joost, and S. Klaus. 2008. 'Uncoupling protein 1 expression in murine skeletal muscle increases AMPK activation, glucose turnover, and insulin sensitivity in vivo', *Physiol Genomics*, 33: 333-40.
Norheim, F., T. M. Langleite, M. Hjorth, T. Holen, A. Kielland, H. K. Stadheim, H. L. Gulseth, K. I. Birkeland, J. Jensen, and C. A. Drevon. 2014. 'The effects of acute and chronic exercise on PGC1alpha, irisin and browning of subcutaneous adipose tissue in humans', *Febs j*, 281: 739-49.
O'Neill, H. M. 2013. 'AMPK and Exercise: Glucose Uptake and Insulin Sensitivity', *Diabetes Metab J*, 37: 1-21.
Oakhill, J. S., Z. P. Chen, J. W. Scott, R. Steel, L. A. Castelli, N. Ling, S. L. Macaulay, and B. E. Kemp. 2010. 'beta-Subunit myristoylation is the gatekeeper for initiating metabolic stress sensing by AMP-activated protein kinase (AMPK)', *Proc Natl Acad Sci U S A*, 107: 19237-41.
Oh, C. M., J. Namkung, Y. Go, K. E. Shong, K. Kim, H. Kim, B. Y. Park, H. W. Lee, Y. H. Jeon, J. Song, M. Shong, V. K. Yadav, G. Karsenty, S. Kajimura, I. K. Lee, S. Park, and H. Kim. 2015. 'Regulation of systemic energy homeostasis by serotonin in adipose tissues', *Nat Commun*, 6: 6794.

Park, A., W. K. Kim, and K. H. Bae. 2014. 'Distinction of white, beige and brown adipocytes derived from mesenchymal stem cells', *World J Stem Cells*, 6: 33-42.

Pavlides, S., I. Vera, R. Gandara, S. Sneddon, R. G. Pestell, I. Mercier, U. E. Martinez-Outschoorn, D. Whitaker-Menezes, A. Howell, F. Sotgia, and M. P. Lisanti. 2012. 'Warburg meets autophagy: cancer-associated fibroblasts accelerate tumor growth and metastasis via oxidative stress, mitophagy, and aerobic glycolysis', *Antioxid Redox Signal*, 16: 1264-84.

Pavlides, S., D. Whitaker-Menezes, R. Castello-Cros, N. Flomenberg, A. K. Witkiewicz, P. G. Frank, M. C. Casimiro, C. Wang, P. Fortina, S. Addya, R. G. Pestell, U. E. Martinez-Outschoorn, F. Sotgia, and M. P. Lisanti. 2009. 'The reverse Warburg effect: aerobic glycolysis in cancer associated fibroblasts and the tumor stroma', *Cell Cycle*, 8: 3984-4001.

Petrovic, N., T. B. Walden, I. G. Shabalina, J. A. Timmons, B. Cannon, and J. Nedergaard. 2010. 'Chronic peroxisome proliferator-activated receptor gamma (PPARgamma) activation of epididymally derived white adipocyte cultures reveals a population of thermogenically competent, UCP1-containing adipocytes molecularly distinct from classic brown adipocytes', *J Biol Chem*, 285: 7153-64.

Picard, F., M. Kurtev, N. Chung, A. Topark-Ngarm, T. Senawong, R. Machado De Oliveira, M. Leid, M. W. McBurney, and L. Guarente. 2004. 'Sirt1 promotes fat mobilization in white adipocytes by repressing PPAR-gamma', *Nature*, 429: 771-6.

Pineda, C. T., S. Ramanathan, K. Fon Tacer, J. L. Weon, M. B. Potts, Y. H. Ou, M. A. White, and P. R. Potts. 2015. 'Degradation of AMPK by a cancer-specific ubiquitin ligase', *Cell*, 160: 715-28.

Pirkmajer, S., S. S. Kulkarni, R. Z. Tom, F. A. Ross, S. A. Hawley, D. G. Hardie, J. R. Zierath, and A. V. Chibalin. 2015. 'Methotrexate promotes glucose uptake and lipid oxidation in skeletal muscle via AMPK activation', *Diabetes*, 64: 360-9.

Polak, P., and M. N. Hall. 2009. 'mTOR and the control of whole body metabolism', *Curr Opin Cell Biol*, 21: 209-18.

Puigserver, P., J. Rhee, J. Donovan, C. J. Walkey, J. C. Yoon, F. Oriente, Y. Kitamura, J. Altomonte, H. Dong, D. Accili, and B. M. Spiegelman. 2003. 'Insulin-regulated hepatic gluconeogenesis through FOXO1-PGC1alpha interaction', *Nature*, 423: 550-5.

Puigserver, P., Z. Wu, C. W. Park, R. Graves, M. Wright, and B. M. Spiegelman. 1998. 'A cold-inducible coactivator of nuclear receptors linked to adaptive thermogenesis', *Cell*, 92: 829-39.

Pulinilkunnil, T., H. He, D. Kong, K. Asakura, O. D. Peroni, A. Lee, and B. B. Kahn. 2011. 'Adrenergic regulation of AMP-activated protein kinase in brown adipose tissue in vivo', *J Biol Chem*, 286: 8798-809.

Pyrzak, B., U. Demkow, and A. M. Kucharska. 2015. 'Brown Adipose Tissue and Browning Agents: Irisin and FGF21 in the Development of Obesity in Children and Adolescents', *Adv Exp Med Biol*, 866: 25-34.

Qi, J., J. Gong, T. Zhao, J. Zhao, P. Lam, J. Ye, J. Z. Li, J. Wu, H. M. Zhou, and P. Li. 2008. 'Downregulation of AMP-activated protein kinase by Cidea-mediated ubiquitination and degradation in brown adipose tissue', *Embo j*, 27: 1537-48.

Qiang, L., L. Wang, N. Kon, W. Zhao, S. Lee, Y. Zhang, M. Rosenbaum, Y. Zhao, W. Gu, S. R. Farmer, and D. Accili. 2012. 'Brown Remodeling of White Adipose Tissue by SirT1-Dependent Deacetylation of Ppargamma', *Cell*, 150: 620-32.

Rodgers, J. T., C. Lerin, W. Haas, S. P. Gygi, B. M. Spiegelman, and P. Puigserver. 2005. 'Nutrient control of glucose homeostasis through a complex of PGC1alpha and SIRT1', *Nature*, 434: 113-8.

Ruan, H. B., M. O. Dietrich, Z. W. Liu, M. R. Zimmer, M. D. Li, J. P. Singh, K. Zhang, R. Yin, J. Wu, T. L. Horvath, and X. Yang. 2014. 'O-GlcNAc transferase enables AgRP neurons to suppress browning of white fat', *Cell*, 159: 306-17.

Ruderman, N. B., X. J. Xu, L. Nelson, J. M. Cacicedo, A. K. Saha, F. Lan, and Y. Ido. 2010. 'AMPK and SIRT1: a long-standing partnership?', *Am J Physiol Endocrinol Metab*, 298: E751-60.

Sahlin, K., M. Tonkonogi, and K. Soderlund. 1998. 'Energy supply and muscle fatigue in humans', *Acta Physiol Scand*, 162: 261-6.

Salih, D. A., and A. Brunet. 2008. 'FoxO transcription factors in the maintenance of cellular homeostasis during aging', *Curr Opin Cell Biol*, 20: 126-36.

Sanchez, A. M., R. B. Candau, A. Csibi, A. F. Pagano, A. Raibon, and H. Bernardi. 2012. 'The role of AMP-activated protein kinase in the coordination of skeletal muscle turnover and energy homeostasis', *Am J Physiol Cell Physiol*, 303: C475-85.

Sanders, M. J., P. O. Grondin, B. D. Hegarty, M. A. Snowden, and D. Carling. 2007. 'Investigating the mechanism for AMP activation of the AMP-activated protein kinase cascade', *Biochem J*, 403: 139-48.

Seale, P. 2015. 'Transcriptional Regulatory Circuits Controlling Brown Fat Development and Activation', *Diabetes*, 64: 2369-75.

Shan, T., X. Liang, P. Bi, and S. Kuang. 2013. 'Myostatin knockout drives browning of white adipose tissue through activating the AMPK-PGC1alpha-Fndc5 pathway in muscle', *Faseb j*, 27: 1981-9.

Subbannayya, Y., N. Syed, M. A. Barbhuiya, R. Raja, A. Marimuthu, N. Sahasrabuddhe, S. M. Pinto, S. S. Manda, S. Renuse, H. C. Manju, M. A. Zameer, J. Sharma, M. Brait, K. Srikumar, J. C. Roa, M. Vijaya Kumar, K. V. Kumar, T. S. Prasad, G. Ramaswamy, R. V. Kumar, A. Pandey, H. Gowda, and A. Chatterjee. 2015. 'Calcium calmodulin dependent kinase kinase 2 - a novel therapeutic target for gastric adenocarcinoma', *Cancer Biol Ther*, 16: 336-45.

Suhane, S., and V. K. Ramanujan. 2011. 'Thyroid hormone differentially modulates Warburg phenotype in breast cancer cells', *Biochem Biophys Res Commun*, 414: 73-8.

Sullivan, J. E., K. J. Brocklehurst, A. E. Marley, F. Carey, D. Carling, and R. K. Beri. 1994. 'Inhibition of lipolysis and lipogenesis in isolated rat adipocytes with AICAR, a cell-permeable activator of AMP-activated protein kinase', *FEBS Lett*, 353: 33-6.

Tang, X., C. C. Lin, I. Spasojevic, E. S. Iversen, J. T. Chi, and J. R. Marks. 2014. 'A joint analysis of metabolomics and genetics of breast cancer', *Breast Cancer Res*, 16: 415.

Uldry, M., W. Yang, J. St-Pierre, J. Lin, P. Seale, and B. M. Spiegelman. 2006. 'Complementary action of the PGC1 coactivators in mitochondrial biogenesis and brown fat differentiation', *Cell Metab*, 3: 333-41.

Valero, T. 2014. 'Mitochondrial biogenesis: pharmacological approaches', *Curr Pharm Des*, 20: 5507-9.

van Dam, A. D., S. Kooijman, M. Schilperoort, P. C. Rensen, and M. R. Boon. 2015. 'Regulation of brown fat by AMP-activated protein kinase', *Trends Mol Med*, 21: 571-9.

van der Vos, K. E., and P. J. Coffer. 2011. 'The extending network of FOXO transcriptional target genes', *Antioxid Redox Signal*, 14: 579-92.

Vander Heiden, M. G., L. C. Cantley, and C. B. Thompson. 2009. 'Understanding the Warburg effect: the metabolic requirements of cell proliferation', *Science*, 324: 1029-33.

Vaziri, H., S. K. Dessain, E. Ng Eaton, S. I. Imai, R. A. Frye, T. K. Pandita, L. Guarente, and R. A. Weinberg. 2001. 'hSIR2(SIRT1) functions as an NAD-dependent p53 deacetylase', *Cell*, 107: 149-59.

Vega, R. B., J. M. Huss, and D. P. Kelly. 2000. 'The coactivator PGC1 cooperates with peroxisome proliferator-activated receptor alpha in transcriptional control of nuclear genes encoding mitochondrial fatty acid oxidation enzymes', *Mol Cell Biol*, 20: 1868-76.

Verdin, E., M. D. Hirschey, L. W. Finley, and M. C. Haigis. 2010. 'Sirtuin regulation of mitochondria: energy production, apoptosis, and signaling', *Trends Biochem Sci*, 35: 669-75.

Vila-Bedmar, R., M. Lorenzo, and S. Fernandez-Veledo. 2010. 'Adenosine 5'-monophosphate-activated protein kinase-mammalian target of rapamycin cross talk regulates brown adipocyte differentiation', *Endocrinology*, 151: 980-92.

Viollet, B., S. Horman, J. Leclerc, L. Lantier, M. Foretz, M. Billaud, S. Giri, and F. Andreelli. 2010. 'AMPK inhibition in health and disease', *Crit Rev Biochem Mol Biol*, 45: 276-95.

Wallace, D. C. 2012. 'Mitochondria and cancer', *Nat Rev Cancer*, 12: 685-98.

Wang, B., X. B. Wang, L. Y. Chen, L. Huang, and R. Z. Dong. 2013. 'Belinostat-induced apoptosis and growth inhibition in pancreatic cancer cells involve activation of TAK1-AMPK signaling axis', *Biochem Biophys Res Commun*, 437: 1-6.

Wang, S., X. Liang, Q. Yang, X. Fu, C. J. Rogers, M. Zhu, B. D. Rodgers, Q. Jiang, M. V. Dodson, and M. Du. 2015. 'Resveratrol induces brown-like adipocyte formation in white fat through activation of AMP-activated protein kinase (AMPK) alpha1', *Int J Obes (Lond)*, 39: 967-76.

Wang, S., P. Song, and M. H. Zou. 2012. 'AMP-activated protein kinase, stress responses and cardiovascular diseases', *Clin Sci (Lond)*, 122: 555-73.

Wang, Y. X., C. L. Zhang, R. T. Yu, H. K. Cho, M. C. Nelson, C. R. Bayuga-Ocampo, J. Ham, H. Kang, and R. M. Evans. 2004. 'Regulation of muscle fiber type and running endurance by PPARdelta', *PLoS Biol*, 2: e294.

Warburg, O., F. Wind, and E. Negelein. 1927. 'THE METABOLISM OF TUMORS IN THE BODY', *J Gen Physiol*, 8: 519-30.

Wareski, P., A. Vaarmann, V. Choubey, D. Safiulina, J. Liiv, M. Kuum, and A. Kaasik. 2009. 'PGC1{alpha} and PGC1{beta} regulate mitochondrial density in neurons', *J Biol Chem*, 284: 21379-85.

Winder, W. W., and D. G. Hardie. 1999. 'AMP-activated protein kinase, a metabolic master switch: possible roles in type 2 diabetes', *Am J Physiol*, 277: E1-10.

Wu, J., P. Bostrom, L. M. Sparks, L. Ye, J. H. Choi, A. H. Giang, M. Khandekar, K. A. Virtanen, P. Nuutila, G. Schaart, K. Huang, H. Tu, W. D. van Marken Lichtenbelt, J. Hoeks, S. Enerback, P. Schrauwen, and B. M. Spiegelman. 2012. 'Beige adipocytes are a distinct type of thermogenic fat cell in mouse and human', *Cell*, 150: 366-76.

Xiao, B., M. J. Sanders, E. Underwood, R. Heath, F. V. Mayer, D. Carmena, C. Jing, P. A. Walker, J. F. Eccleston, L. F. Haire, P. Saiu, S. A. Howell, R. Aasland, S. R. Martin, D. Carling, and S. J. Gamblin. 2011. 'Structure of mammalian AMPK and its regulation by ADP', *Nature*, 472: 230-3.

Xin, C., J. Liu, J. Zhang, D. Zhu, H. Wang, L. Xiong, Y. Lee, J. Ye, K. Lian, C. Xu, L. Zhang, Q. Wang, Y. Liu, and L. Tao. 2016. 'Irisin improves fatty acid oxidation and glucose utilization in type 2 diabetes by regulating the AMPK signaling pathway', *Int J Obes (Lond)*, 40: 443-51.

Yadav, N., and D. Chandra. 2013. 'Mitochondrial DNA mutations and breast tumorigenesis', *Biochim Biophys Acta*, 1836: 336-44.

Ye, L., J. Wu, P. Cohen, L. Kazak, M. J. Khandekar, M. P. Jedrychowski, X. Zeng, S. P. Gygi, and B. M. Spiegelman. 2013. 'Fat cells directly sense temperature to activate thermogenesis', *Proc Natl Acad Sci U S A*, 110: 12480-5.

Yoon, J. C., P. Puigserver, G. Chen, J. Donovan, Z. Wu, J. Rhee, G. Adelmant, J. Stafford, C. R. Kahn, D. K. Granner, C. B. Newgard, and B. M. Spiegelman. 2001. 'Control of hepatic gluconeogenesis through the transcriptional coactivator PGC1', *Nature*, 413: 131-8.

Yu, J., and J. Auwerx. 2009. 'The role of sirtuins in the control of metabolic homeostasis', *Ann N Y Acad Sci*, 1173 Suppl 1: E10-9.

Zhu, M., J. Miura, L. X. Lu, M. Bernier, R. DeCabo, M. A. Lane, G. S. Roth, and D. K. Ingram. 2004. 'Circulating adiponectin levels increase in rats on caloric restriction: the potential for insulin sensitization', *Exp Gerontol*, 39: 1049-59.

Zou, M. H., X. Y. Hou, C. M. Shi, S. Kirkpatick, F. Liu, M. H. Goldman, and R. A. Cohen. 2003. 'Activation of 5'-AMP-activated kinase is mediated through c-Src and phosphoinositide 3-kinase activity during hypoxia-reoxygenation of bovine aortic endothelial cells. Role of peroxynitrite', *J Biol Chem*, 278: 34003-10.

Zou, M. H., C. Shi, and R. A. Cohen. 2002. 'High glucose via peroxynitrite causes tyrosine nitration and inactivation of prostacyclin synthase that is associated with

thromboxane/prostaglandin H(2) receptor-mediated apoptosis and adhesion molecule expression in cultured human aortic endothelial cells', *Diabetes*, 51: 198-203.

12. PUBLICATION LIST (approved by the Kenézy Life Science Library)

UNIVERSITY of DEBRECEN

UNIVERSITY AND NATIONAL LIBRAY
UNIVERSITY OF DEBRECEN
H-4002 Egyetem tér 1, Debrecen
Phone: +3652/410-443, email: publikaciok@lib.unideb.hu

Registry number: DEENK/1/2018.PL
Subject: PhD Publikációs Lista

Candidate: Tamás Fodor
Neptun ID: WAN836
Doctoral School: Doctoral School of Molecular Medicine
MTMT ID: 10043604

List of publications related to the dissertation

1. Abdul-Rahman, O., Kristóf, E., Doan-Xuan, Q. M., Vida, A., Nagy, L., Horváth, A., Simon, J., Maros, T. M., Szentkirályi, I., Palotás, L., Debreceni, T., Csizmadia, P., Szerafin, T., **Fodor, T.**, Szántó, M., Tóth, A., Kiss, B. K., Bacsó, Z., Bai, P.: AMP-Activated Kinase (AMPK) Activation by AICAR in Human White Adipocytes Derived from Pericardial White Adipose Tissue Stem Cells Induces a Partial Beige-Like Phenotype.
PLoS One. 11 (6), e0157644, 2016.
DOI: http://dx.doi.org/10.1371/journal.pone.0157644
IF: 2.806

2. **Fodor, T.**, Szántó, M., Abdul-Rahman, O., Nagy, L., Dér, Á., Kiss, B. K., Bai, P.: Combined Treatment of MCF-7 Cells with AICAR and Methotrexate, Arrests Cell Cycle and Reverses Warburg Metabolism through AMP-Activated Protein Kinase (AMPK) and FOXO1.
PLoS One. 11 (2), 1-16, 2016.
DOI: http://dx.doi.org/10.1371/journal.pone.0150232
IF: 2.806

DEBRECENI EGYETEM
KENÉZY ÉLETTUDOMÁNYI EGYETEMI ÉS NEMZETI KÖNYVTÁRA

UNIVERSITY AND NATIONAL LIBRAY
UNIVERSITY OF DEBRECEN
H-4002 Egyetem tér 1, Debrecen
Phone: +3652/410-443, email: publikaciok@lib.unideb.hu

List of other publications

3. Mikó, E., Kovács, T., **Fodor, T.**, Bai, P.: Methods to assess to role of poly(ADP-ribose) polymerases in regulating mitochondrial oxidation.
Methods Mol. Biol. 1608, 185-200, 2017.

4. Márton, J., **Fodor, T.**, Nagy, L., Vida, A., Kis, G., Brunyánszki, A., Antal, M., Lüscher, B., Bai, P.: PARP10 (ARTD10) modulates mitochondrial function.
PLoS One. "Accepted by Publisher", 2017.
IF: 2.806 (2016)

5. Bai, P., Nagy, L., **Fodor, T.**, Liaudet, L., Pacher, P.: Poly(ADP-ribose) polymerases as modulators of mitochondrial activity.
Trends Endocrinol. Metab. 26 (2), 75-83, 2015.
DOI: http://dx.doi.org/10.1016/j.tem.2014.11.003
IF: 8.964

6. Szántó, M., Brunyánszki, A., Márton, J., Vámosi, G., Nagy, L., **Fodor, T.**, Kiss, B. K., Virág, L., Gergely, P., Bai, P.: Deletion of PARP-2 induces hepatic cholesterol accumulation and decrease in HDL levels.
Biochim. Biophys. Acta-Mol. Basis Dis. 1842 (4), 594-602, 2014.
DOI: http://dx.doi.org/10.1016/j.bbadis.2013.12.006
IF: 4.882

7. Nagy, D., Gönczi, M., Dienes, B., Szöőr, Á., Fodor, J., Nagy, Z., Tóth, A., **Fodor, T.**, Bai, P., Szűcs, G., Rusznák, Z., Csernoch, L.: Silencing the KCNK9 potassium channel (TASK-3) gene disturbs mitochondrial function, causes mitochondrial depolarization, and induces apoptosis of human melanoma cells.
Arch. Dermatol. Res. 306 (10), 885-902, 2014.
DOI: http://dx.doi.org/10.1007/s00403-014-1511-5.
IF: 1.902

Total IF of journals (all publications): 24,166
Total IF of journals (publications related to the dissertation): 5,612

The Candidate's publication data submitted to the iDEa Tudóstér have been validated by DEENK on the basis of Web of Science, Scopus and Journal Citation Report (Impact Factor) databases.

03 January, 2018

13. AKNOWLEDGEMENT

First of all I would like express my sincere gratitude to my supervisor, Dr. Péter Bay, for helping and guiding my work and for the continuous support and motivation during my Ph.D. study. I am grateful that he gave me the opportunity to learn and work in his research group.

I would like to thank to Prof. László Virág, head of Department of Medical Chemistry and Prof. Pál Gergely for giving me the opportunity to work at the Department.

Many thanks to all the people in the Department of Medical Chemistry, especially to our group: András Vida, Judit Márton, Lilla Nagy, Dr. Edit Mikó, Tünde Kovács.

I am also thankful to my former colleague Omar Abdul Rahman for his help on the experiments related to human adipocyte browning.

I am very grateful to Adrienn Sipos for her continuous scientific support and friendship.

I also would like to thank László Finta, Ms. Erzsébet Herbály for their excellent technical assistance.

Most importantly and dearly, I would like to thank to my beloved wife and family and to all of my dear friends helping me get through the difficult times, and for their continuous encouragement during my PhD study.

14. KEYWORDS

AMPK, breast cancer, mitochondria, mitochondrial biogenesis, Warburg effect, adipocyte, beige, browning, thermogenesis, SIRT1, PGC1α, FOXO1, UCP1

KULCSSZAVAK

AMPK, emlőrák, mitokondrium, mitokondriális biogenezis, Warburg hatás, adipocita, beige, browning, termogenezis, SIRT1, PGC1α, FOXO1, UCP1

The work/publication is supported by the GINOP- 2.3.2-15-2016-00006 project. The project is co-financed by the European Union and the European Regional Development Fund.

15. APPENDIX

The thesis is based on the following publications: